

CHAPTER 5

Probabilistic design tools and applications

5.1 INTRODUCTION

In this chapter the probabilistic design tools will be presented. This encompasses the methods to combine the inherent uncertainty of the natural boundary conditions, the uncertainty due to lack of information of the natural environment, the quality of the structure and the engineering models into the measure of a failure probability that expresses the reliability of a structural system. Also a decision has to be taken whether the structural reliability is sufficient in view of the economic and societal functions of the structure. As an aid to this decision a safety philosophy has been formulated.

As the application of the probabilistic design method requires considerable effort and resources, a simpler approach using partial safety factors is derived within the probabilistic framework.

This chapter aims at designers of vertical breakwaters with an interest in the probabilistic design method and the background of a partial safety factor code. It may also serve as an introduction for researchers who want to familiarise themselves with the theoretical backgrounds. These readers however, are referred to Volume II for more detailed information.

This chapter treats the description of the failure modes of a vertical breakwater including the uncertainties in section 5.2.2 and 5.3.2 and the methods to calculate the probabilities of failure of each failure mode in section 5.2.3. In section 5.2.4 the methods to gain insight in the performance of the structure as a whole are treated. The ways to combine the failure probabilities of the various modes into the reliability of the structure are given in section 5.2.5.

The framework to decide on the optimal failure probability is dealt with in section 5.2.6 together with the partial safety factor system. In section 5.4 the theory is applied to a number of case studies. Finally, some perspectives are given in section 5.5.

5.2 GENERAL INTRODUCTION OF PROBABILISTIC METHODS

5.2.1 *Introduction*

The most important and most clear difference of probabilistic design compared to conventional (deterministic) design is that in probabilistic design one takes explicitly account of the uncertainties involved in the behaviour of the structure under consideration. Over the years considerable progress has been made in the development of probabilistic methods. This section attempts to introduce shortly the probabilistic working method, independent of the application to vertical breakwaters. For further reading, several textbooks have been written. As a start for further reading the following references can be used:

- Thoft-Christensen & Baker, 1982;
- Madsen, et al. 1986;
- Ditlevsen & Madsen, 1996.

Mentioning these three references is in no way meant to imply any judgement of the value of other references on the same subject.

5.2.2 *Limit state equations and uncertainties*5.2.2.1 *The concept of limit states*

The first step in a reliability analysis of any structure is defining its functions. When the functions of the structure are defined, the ways in which malfunctioning of the structure can occur are defined. These ways of malfunctioning are called failure modes. The failure modes are described in such a way that they are fit for mathematical treatment. A function that describes functioning or failure of a structure or one of its components is called a reliability function or limit state equation. A general limit state equation is denoted g and can be written as:

$$M = g(\mathbf{X}) = R(\mathbf{X}) - S(\mathbf{X}) \quad (5-1)$$

In which \mathbf{X} is a vector of random variables describing the geometry of the structure, the loads that are applied, the strength of materials etc; M is a random variable, usually referred to as the safety margin; $R(\mathbf{X})$ is the strength (Resistance) of the structure as a function of \mathbf{X} ; $S(\mathbf{X})$ is the load (Solicitation) on the structure as a function of \mathbf{X} .

The limit state equations are defined in such a way that negative values of realisations of M indicate failure and positive values indicate safe states.

For a general structure several limit states can be defined. Take for example the statically determined concrete beam with a point load in the middle in Figure 5-1.

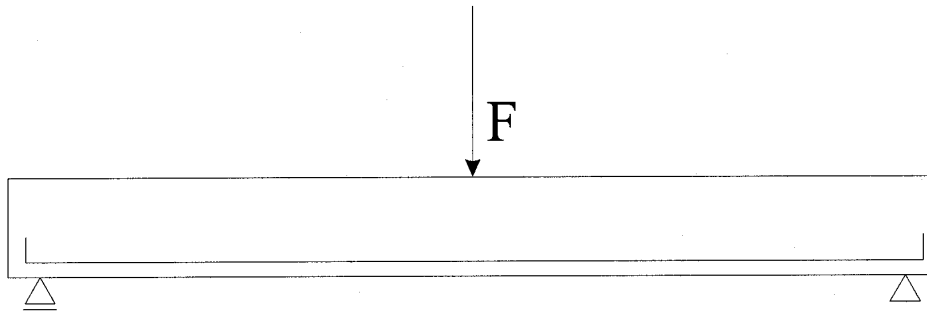


Figure 5-1. Statically determined concrete beam.

In the situation where the position of the load is fixed, the following limit states can be defined for this simple structure:

- Exceedance of the ultimate bending moment in the middle of the beam;
- Exceedance of the shearing strength near one of the supports;
- Exceedance of the admissible deformation in the middle of the beam;
- Cracking of the concrete on the lower side of the beam, which may lead to corrosion of the reinforcement bars in an aggressive environment;
- Chloride ingress through the uncracked concrete, followed by corrosion of the reinforcement.

Observation of these five failure modes shows that the consequences are not of equal magnitude in all cases. The first two failure modes lead to immediate collapse of the beam, while the other three threaten its functioning (inadmissible deformation) or may introduce failure after a period of time in which repair can still be made (cracking and chloride ingress).

Therefore, in general four kinds of limit states are defined (see e.g. Eurocode 1, Basis of Design, 1994):

- Ultimate Limit States (ULS), describing immediate collapse of the structure;
- Serviceability Limit States (SLS), describing loss of function of the structure without collapse (a beam with a too large deformation might not be able to support a load which is sensitive to this deformation, while the beam is still able to withstand the load);
- Accidental Limit States (ALS), describing failure under accident conditions (collisions, explosions).

The acceptable probability of failure for a certain limit state depends on its character. Usually the highest safety requirements are set for Ultimate Limit States. Accepted failure probabilities for Serviceability Limit States might be considerably higher, especially if the effects of failure are easily reversed. Accidental Limit States can be treated like Ultimate Limit States, or the probability of occurrence of the accident can be taken into account. The acceptable probability of failure also depends on the time in which it is possible that a certain failure mode occurs. For failure during the construction phase, this time is considerably shorter than for the other types of failure. Therefore, for the construction phase characteristic values with a smaller return period are defined.

5.2.2.2 *Uncertainties related to the limit state formulation*

Basically, the limit state equation is a deterministic model indicating functioning or failure of the structure. Uncertainties are generally related to the input of the limit state equation. The following types of uncertainty are discerned (see also Vrijling & van Gelder, 1998):

1. Inherent uncertainty;
2. Model uncertainty;
3. Statistical uncertainty.

Ad 1: The uncertainty that is part of the described physical process is called inherent uncertainty. This uncertainty exists even if unlimited data is available. For instance: even if the wave height at a certain location is measured during an infinite period of time, the wave heights will still be uncertain in the future. A probability distribution can be used to describe the inherent uncertainty.

Ad 2: Model uncertainty can be distinguished into two subtypes. The first type of model uncertainty is related to the limit state equation itself. The model describing the physical process is a schematisation of the true process. Due to the schematisation, parts of the process are left out under the assumption that they are not important to the final result. This leaving out of parts of the process introduces a scatter (uncertainty) when comparing the model to measurements. Using a more sophisticated model, which describes more accurately the physical process, can reduce this type of uncertainty. The second kind of model uncertainty is related to the distribution function of the input variables. Also parametric distribution functions are schematisations of some real (unknown) distribution. Model uncertainty related to the input variables means that the chosen model might not be the true or best model. This type of uncertainty is reduced if more measurements are available, since then the correct distribution type becomes more clear.

Ad 3: When fitting a parametric distribution to limited data, the parameters of the distribution are also of random nature. The uncertainty in the parameters is generally referred to as statistical uncertainty. This type of uncertainty reduces when the number of data points increases.

5.2.3 Reliability analysis on level II and III

5.2.3.1 Introduction

The reliability of a structure or component is defined as the probability that the structure or component is able to fulfil its function. Reversibly the probability of failure is defined as the probability that the structure does not function. The properties of the structure (load, strength, geometry) are modelled by a vector of random variables, called the basic variables. The space of the basic variables is divided in a safe set and a failure set by the limit state equation(s) (Figure 5-2).

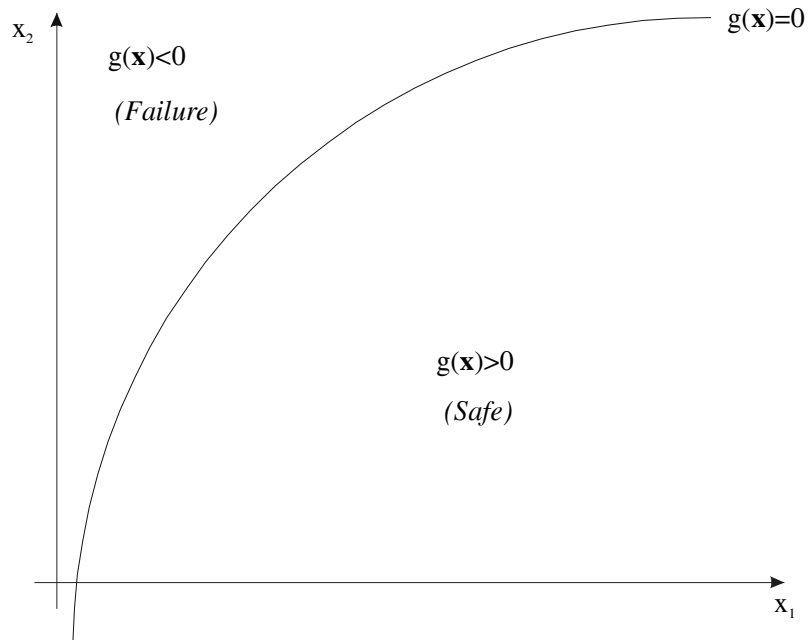


Figure 5-2. Limit state equation, safe set and failure set in the space of basic variables.

The probability of failure equals the probability that a combination of values of the basic variables lies in the failure domain. In formula:

$$P_f = P(\mathbf{X} \in F) \tag{5-2}$$

In which \mathbf{X} is the vector of basic variables; and F is the failure domain.

Evaluation of this probability comes down to the determination of the volume of the joint probability density function of the basic variables in the failure domain. In formula:

$$P_f = \int_F f_{\mathbf{x}}(\mathbf{x}) d\mathbf{x} = \int_{g(\mathbf{x}) \leq 0} f_{\mathbf{x}}(\mathbf{x}) d\mathbf{x} \quad (5-3)$$

In which $f_{\mathbf{x}}(\mathbf{x})$ is the joint probability density function of the basic variables; and $g(\mathbf{x})$ is the limit state equation.

In general it is not possible to solve the integral analytically. Several numerical methods have been developed in the past. Section 5.2.3.2 introduces the direct integration methods. Section 5.2.3.3 introduces approximating methods. More details are given in (Thoft-Christensen & Baker, 1982; Madsen et al. 1986; Ditlevsen & Madsen, 1996).

5.2.3.2 Direct integration methods (Level III)

Riemann integration

Standard numerical integration methods can be applied to Equation (5-3). In that case the probability of failure is estimated by:

$$P_f \approx \sum_{i_1=0}^{m_1} \sum_{i_2=0}^{m_2} \dots \sum_{i_n=0}^{m_n} 1(g(\mathbf{x})) f_{\mathbf{x}}(x_{01} + i_1 \Delta x_1, x_{02} + i_2 \Delta x_2, \dots, x_{0n} + i_n \Delta x_n) \Delta x_1 \Delta x_2 \dots \Delta x_n \quad (5-4)$$

In which m_i is the number of steps for variable number i ; n is the number of basic variables; $1(g(\mathbf{x}))$ is the indicator function defined as

$$1(g(\mathbf{x})) = 1, \quad \text{if } g(\mathbf{x}) \leq 0; \quad (5-5)$$

$$1(g(\mathbf{x})) = 0, \quad \text{if } g(\mathbf{x}) > 0 \quad (5-6)$$

The calculation time depends on the number of basic variables (n) and the number of calculation steps to be taken (m). The total number of iterations can be written as:

$$N = \prod_{j=1}^n m_j \quad (5-7)$$

This indicates that the calculation time increases rapidly with an increasing number of basic variables. Furthermore the calculation time as well as the accuracy of the method depend strongly on the number of calculation steps per variable. Importance sampling methods have been proposed to increase the calculation speed as well as the accuracy of the calculation method. These methods are

not elaborated upon here. Reference is made to (Ouypornprasert, 1987; CUR, 1997).

Monte Carlo simulation

A different method which uses the joint distribution of the basic variables is Monte Carlo simulation. In this method a large sample of values of the basic variables is generated and the number of failures is counted. The number of failures equals:

$$N_f = \sum_{j=1}^N 1(g(\mathbf{x}_j)) \quad (5-8)$$

In which N is the total number of simulations. In Equation (5-8) the same indicator function is used as in Equation (5-4).

The probability of failure can be estimated by:

$$P_f \approx \frac{N_f}{N} \quad (5-9)$$

The coefficient of variation of the failure probability can be estimated by:

$$V_{P_f} \approx \frac{1}{\sqrt{P_f N}} \quad (5-10)$$

In which P_f denotes the estimated failure probability.

The accuracy of the method depends on the number of simulations (CUR, 1997). The relative error made in the simulation can be written as:

$$\varepsilon = \frac{\frac{N_f}{N} - P_f}{P_f} \quad (5-11)$$

The expected value of the error is zero. The standard deviation is given as:

$$\sigma_\varepsilon = \sqrt{\frac{1 - P_f}{NP_f}} \quad (5-12)$$

For a large number of simulations, the error is Normal distributed. Therefore the probability that the relative error is smaller than a certain value E can be written as:

$$P(\varepsilon < E) = \Phi\left(\frac{E}{\sigma_\varepsilon}\right) \quad (5-13)$$

$$N > \frac{k^2}{E^2} \left(\frac{1}{P_f} - 1 \right) \quad (5-14)$$

The probability of the relative error E being smaller than $k\sigma_\varepsilon$ now equals $\Phi(k)$. For desired values of k and E the required number of simulations is given by:

Requiring a relative error of $E = 0.1$ lying within the 95 % confidence interval ($k = 1.96$) results in:

$$N > 400 \left(\frac{1}{P_f} - 1 \right) \quad (5-15)$$

Equations (5-14) and (5-15) show that the required number of simulations and thus the calculation time depend on the probability of failure to be calculated. Most structures in coastal engineering possess a relatively high probability of failure (i.e. a relatively low reliability) compared to structural elements/systems, resulting in reasonable calculation times for Monte Carlo simulation. The calculation time is independent of the number of basic variables and therefore Monte Carlo simulation should be favoured over the Riemann method in case of a large number of basic variables (typically more than five). Furthermore, the Monte Carlo method is very robust, meaning that it is able to handle discontinuous failure spaces and reliability calculations in which more than one design point are involved (see below).

The problem of long calculation times can be partly overcome by applying importance sampling. This is not elaborated upon here. Reference is made to (Bucher, 1987; Ditlevsen & Madsen, 1996; CUR, 1997).

5.2.3.3 *Approximating methods (Level II)*

First Order Reliability Method (FORM)

In the FORM-procedure the value of the volume integral (Equation (5-3)) is estimated by an approximating procedure. The following procedure is followed to estimate the probability of failure:

- A transformation $\mathbf{X} = T(\mathbf{U})$ is carried out, mapping all the random variables in the space of standard normal-distributed variables (U -space);
- The reliability function is also transformed to the U -space and is replaced by its first-order Taylor approximation in a certain point;

Hasofer & Lind (1974) have shown that the calculated probability of failure is invariant for the formulation of the limit state equation, if the limit state is linearised in the point with the highest value of the joint probability density of the basic variables (design point, see Fig. 5-3).

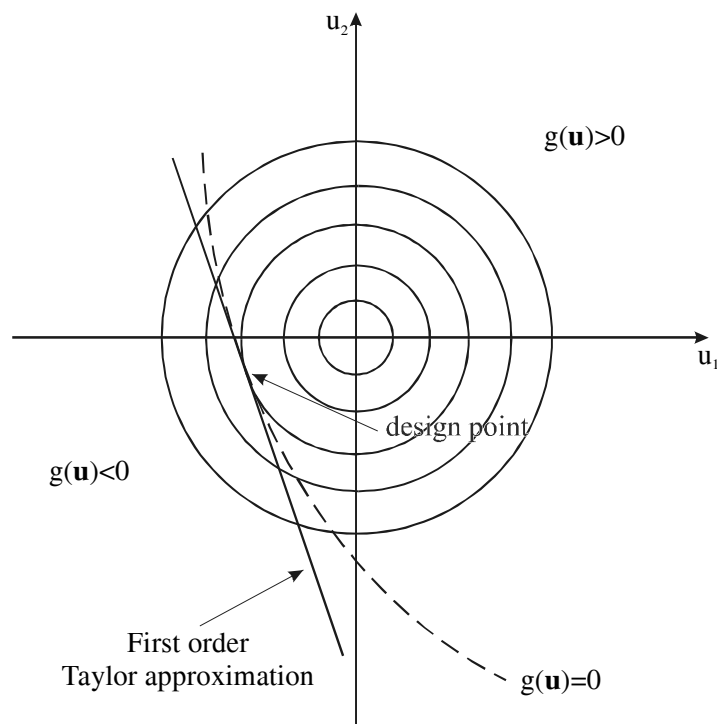


Figure 5-3: Design point, real failure boundary and linearised failure boundary in the space of the standard-normal variables (U -space)

In the U -space this point coincides with the point at the failure boundary with minimum distance to the origin. This distance is called the Hasofer-Lind reliability index (β_{HL}). For the calculation of the reliability index several methods have been proposed. Reference is made to (Thoft-Christensen & Baker, 1982; Madsen et al. 1986; Ditlevsen & Madsen, 1996). As a result of the transformation to U -space, the safety margin $M = g(\mathbf{x})$ is linearised in U -space. Therefore, the probability of failure can be approximated by:

$$P_f = P(M < 0) \approx P(\beta_{HL} - \boldsymbol{\alpha}^T \mathbf{U}) = \Phi(-\beta_{HL}) \quad (5-16)$$

This solution is exact only if the reliability function is linear in the basic variables and if the basic variables have Normal distributions. As noted above, the elements in the $\boldsymbol{\alpha}$ -vector are a measure of the importance of the random variables. $\alpha_i^2 \cdot 100\%$ gives the relative importance in % of the random variable x_i .

Generally, the limit state equation is dependent on a number of deterministic parameters, which can be collected in the vector \mathbf{p} . The elements in \mathbf{p} can be statistical parameters like expected values and standard deviations and it can be e.g. geometrical quantities with negligible uncertainty. The limit state equation in U -space is written as:

$$g(\mathbf{U}, \mathbf{p}) = 0 \quad (5-17)$$

For the reliability index β_{HL} the sensitivity with respect to the parameter p_j can easily be obtained in the form, see e.g. Madsen et al (1986):

$$\frac{d\beta_{HL}}{dp_j} \quad (5-18)$$

FORM calculations generally provide estimates of the failure probability in relatively short calculation times. This is a big advantage over level III methods in general. However, if the reliability function is highly non-linear, FORM-estimates of P_f may possess a considerable error. In Figure 5-3 a curved limit state equation is shown together with its first order approximation. In this case the estimate of the probability of failure obtained with FORM underestimates the real failure probability. In case of discontinuous failure spaces, FORM procedures may fail to give a correct failure probability at all.

Second Order Reliability Method (SORM)

The disadvantages of FORM estimates are partly overcome by the Second Order Reliability Method (SORM). Instead of calculating the probability of failure directly from the reliability index, a formula is applied in which the curvature of the limit state equation at the design point is used to get a better estimate of the probability of failure. This working method implies that a reliability index and a design point are known. Therefore, in SORM at first a FORM calculation is performed. For more details reference is made to (Breitung, 1984). Regarding the description of discontinuous failure spaces, the same disadvantages as for FORM apply.

5.2.4 *Fault tree analysis*

5.2.4.1 *General system analysis by fault tree*

The methods for reliability calculations given in the previous section are all based on the analysis of one limit state only. However, even for a very simple structure generally several failure modes are relevant. A set of limit states can be presented as a series system, a parallel system or a combination thereof. The probability of failure of the system is determined by the properties of the system as well as by the individual failure probabilities of the components (limit states).

If the order of occurrence of the failure modes is not of consequence for the failure of the structure, the system of failure modes can be described by a fault tree. An example is given in Figure 5-4. The system representation is also given.

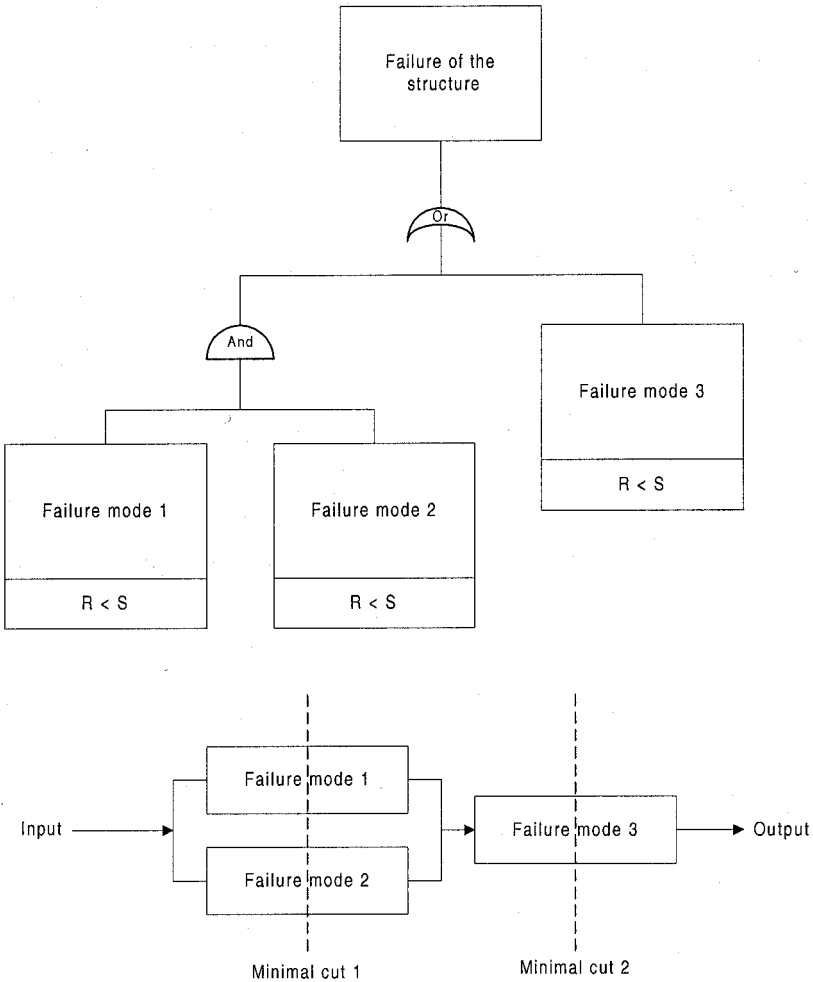


Figure 5-4. Fault tree and system representation of a system of three failure modes.

The two presentations of the system are completely equivalent. An and-gate coincides with a parallel system of failure modes and an or-gate coincides with a series system of failure modes.

An overview of the notation used in the fault trees is given in Table 5-1 and Table 5-2.

Table 5-1. Overview of gate symbols in fault trees (Andrews & Moss, 1993).

Symbol	Description
	"And" gate
	"Or" gate
	Voting gate
	Inhibit gate
	Exclusive "or" gate
	Priority "and" gate

Table 5-2. Overview of event symbols in fault trees (Andrews & Moss, 1993).

Symbol	Description
	Base event
	Event not further developed in the tree
	Compound event I
	Compound event II
	Conditional event (used in combination with inhibit gate)
	Normal event (house event)
	Reference symbol

5.2.5 Calculation of system probability of failure

5.2.5.1 Introduction

In the previous section the fault tree presentation of a system of failure modes is introduced. The fault tree indicates whether failure modes are part of a parallel system or part of a series system of failure modes. An analytical expression for the probability of system failure is possible only if the failure modes are uncorrelated or fully correlated. The formulae are given in Table 5-3.

Table 5-3. Overview of system probability of failure for combinations of correlation and system type.

System type	Upper bound	Independent components	Lower bound
Series	$P_f = \sum_{i=1}^n P_{f_i}$	$P_f = \prod_{i=1}^n P_{f_i}$	$P_f = \max(P_{f_i})$
Parallel	$P_f = \min(P_{f_i})$	$P_f = 1 - \prod_{i=1}^n (1 - P_{f_i})$	$P_f = 0$

The formulae given in Table 5-3 are also bounds on the real system probability of failure. For a series system the upper bound is given by the uncorrelated case and the lower bound by the case with full correlation. For a parallel system the upper bound is given by the case with full correlation and the lower bound by the uncorrelated case.

For arbitrary correlation between limit state equations, an analytical solution is no longer possible. In that case one has to use numerical methods to obtain the system probability of failure. Section 5.2.5.2 introduces direct integration methods. Section 5.2.5.3 introduces a few approximating methods for system failure.

5.2.5.2 Direct integration methods for systems

Riemann integration

The Riemann process introduced in section 5.2.3.2 can also be applied to evaluate the probability of system failure. Similar to the case with one limit state equation the probability of failure is estimated by:

$$P_f \approx \sum_{i_1=0}^{m_1} \sum_{i_2=0}^{m_2} \dots \sum_{i_n=0}^{m_n} \mathbf{1}(\mathbf{g}(\mathbf{x})) f_{\mathbf{x}}(x_{01} + i_1 \Delta x_1, x_{02} + i_2 \Delta x_2, \dots, x_{0n} + i_n \Delta x_n) \Delta x_1 \Delta x_2 \dots \Delta x_n \quad (5-19)$$

In which $\mathbf{g}(\mathbf{x})$ is a vector of limit state equations; m_i is the number of steps for variable number i ; and n is the number of basic variables.

Since now the system probability of failure has to be calculated, the indicator function is defined in a different way. For a series system the indicator function is given as:

$$\mathbf{1}(\mathbf{g}(\mathbf{x})) = \begin{cases} 1 & \text{if } \min_{i=1,n} (g_i(\mathbf{x})) \leq 0 \\ 0 & \text{if } \min_{i=1,n} (g_i(\mathbf{x})) > 0 \end{cases} \quad (5-20)$$

For a parallel system the indicator function is:

$$1(\mathbf{g}(\mathbf{x})) = \begin{cases} 1 & \text{if } \max_{i=1,n}(g_i(\mathbf{x})) \leq 0 \\ 0 & \text{if } \max_{i=1,n}(g_i(\mathbf{x})) > 0 \end{cases} \quad (5-21)$$

In general the evaluation of more limit state equations in a calculation step will not take much extra time. Therefore, the performance of the Riemann integration for more limit states is comparable to the performance for one limit state (section 5.2.3.2).

Monte Carlo simulation

Like Riemann integration, Monte Carlo simulation is also applicable for systems. The number of failures is determined by applying Equation (5-8). Also in this case the indicator function is replaced by one of the system indicator functions given in the previous section. The evaluation of extra limit states is in general not very time consuming. Therefore, the performance of the Monte Carlo method is not heavily influenced by the application to more limit states. Also for systems the Monte Carlo method proves to be a very robust, but not very fast method.

5.2.5.3 *Approximating methods for systems*

Fundamental bounds on the system probability of failure

When the failure probabilities per limit state are known, it is always possible to provide a lower and upper bound for the failure probability (see Table 5-3). In several cases these bounds prove to give a reasonable range in which the real probability of system failure is to be found. In some cases however, the fundamental bounds provide a too wide range. In that case one has to use more advanced methods.

Ditlevsen bounds for the system probability of failure

An alternative calculation method for the bounds of the probability of failure of a series system is developed by (Ditlevsen, 1979). The bounds according to Ditlevsen are given by:

$$P(g_1(\bar{x}) < 0) + \sum_{i=2}^n \max \left[\left(P(g_i(\bar{x}) < 0) - \sum_{j=1}^{i-1} P(g_i(\bar{x}) < 0 \cap g_j(\bar{x}) < 0) \right), 0 \right] \leq P_f \quad (5-22)$$

$$P_f \leq \sum_{i=1}^n P(g_i(\bar{x}) < 0) - \max_{j < i} (P(g_i(\bar{x}) < 0 \cap g_j(\bar{x}) < 0))$$

These bounds are more narrow than the fundamental bounds, but for a large number of limit states they may still be too wide.

First-order method for systems

An approximating procedure which is able to provide a more accurate estimate of the system probability of failure of a system is proposed by (Hohenbichler & Rackwitz, 1983). In this method the correlated limit state equations are transformed to a set of uncorrelated limit states. The system probability of failure can then be calculated using fundamental rules for the probability of system failure and first or second order estimates of the probability of failure per limit state. Generally, an approximation is obtained for $\Phi_n(\boldsymbol{\beta}, \boldsymbol{\rho})$ in which $\boldsymbol{\beta}$ denotes the vector of reliability indices for every limit state and $\boldsymbol{\rho}$ denotes the correlation between the failure modes. The failure probability of a parallel system is then given by:

$$P_{f;parallel} \approx \Phi_n(-\boldsymbol{\beta}, \boldsymbol{\rho}) \quad (5-23)$$

And for a series system by:

$$P_{f;series} \approx 1 - \Phi(\boldsymbol{\beta}, \boldsymbol{\rho}) \quad (5-24)$$

This method in general has shorter calculation times than the level III methods. However, due to the approximations estimates of the failure probability might show considerable errors (Schuëller & Stix, 1987). As with all approximating methods one should be aware of this disadvantage.

5.2.6 *Choice of safety level*

To construct a breakwater that is always performing its function and is perfectly safe from collapse is at least an uneconomical pursuit and most likely an impossible task. Although expertly designed and well constructed, there will always be a small possibility that the structure fails under severe circumstances (Ultimate Limit State). The acceptable probability of failure is a question of socio-economic reasoning.

In a design procedure one has to determine the preferred level of safety (i.e. the acceptable failure probability). For most civil engineering structures the acceptable failure probability will be based on considerations of the probability of loss of life due to failure of the structure.

In general two points of view for the acceptable safety level can be defined (Vrijling et al., 1995):

The individual accepted risk. The probability accepted by an individual person to die in case of failure of the structure; In Western countries this probability is of the order 10^{-4} per year or smaller

The societal accepted risk. Two approaches are presented, depending on the relative importance of the total number of lives lost in case of failure on the one hand and the total economic damage on the other. If the number of potential casualties is large the likelihood of failure should be limited accordingly. The accepted probability of occurrence of a certain number of casualties in case of failure of a structure is then restricted proportional to the inverse of the square of this number (Vrijling et al., 1995). If the economic damage is large, an economic optimisation equating the marginal investment in the structure with the marginal reduction in risk should be carried out to find the optimal dimensions of the structure.

The two boundary conditions based on the loss of human lives form the upper limits for the acceptable probability of failure of any structure. In case of a breakwater without amenities the probability of loss of life in case of failure is very small. In that case the acceptable probability of failure can be determined by economical optimisation, weighing the expected value of the capitalised damage in the life of the structure (risk) against the investment in the breakwater. The next section provides more background on this concept.

If, for a specific breakwater, failure would include a number of casualties, the economic optimisation should be performed under the constraint of the maximum allowable probability of failure as defined by the two criteria related to loss of life.

The explicit assessment of the acceptable probability of failure as sketched above is only warranted in case of large projects with sufficient means. For smaller projects a second approach is generally advised. This second approach to the acceptable safety level is based on the evaluation of the safety of existing structures supplemented by considerations of the extent of the losses involved in case of failure. Consequently the assumption is made that the new structure should meet the safety requirements that seem to be reasonable in practice. This approach is found in many codes where a classification of the losses in case of failure leads to an acceptable probability of failure. Most structural codes provide safety classes for structures (NKB 1978, Eurocode 1). The structure to be designed might fit in one of these safety classes providing an acceptable probability of failure. It should be noted however that for most structural systems loss of life is involved contrary to breakwaters. Therefore the following classification and table with acceptable probabilities of failure was developed especially for vertical breakwaters:

- ◆ *Very low safety class*, where failure implies no risk to human injury and very small environmental and economic consequences

- ◆ *Low safety class*, where failure implies no risk to human injury and some environmental and economic consequences
- ◆ *Normal safety class*, where failure implies risk to human injury and significant environmental pollution or high economic or political consequences
- ◆ *High safety class*, where failure implies risk to human injury and extensive environmental pollution or very high economic or political consequences

Table 5-4. Overview of safety classes.

Limit state type	Safety class			
	Low	Normal	High	Very high
SLS	0.4	0.2	0.1	0.05
ULS	0.2	0.1	0.05	0.01

5.2.7 Reliability based design procedures

5.2.7.1 General formulation of reliability based optimal design

Generally, in a design process one pursues the cheapest design that fulfils the demands defined for the structure. The demands can be expressed in two fundamentally different ways:

- The total expected lifetime costs of the structure consisting of the investment and the expected value of the damage costs are minimised as a function of the design variables;
- If a partial safety factor system is available, one can optimise the design by minimising the construction costs as a function of the design variables under the constraint that the design equations related to the limit state equations for all the failure modes are positive.

The minimisation of the lifetime costs can be formalised as follows (Enevoldsen & Sørensen, 1993):

$$\begin{aligned}
 \min_{\mathbf{z}} C_T(\mathbf{z}) &= C_I(\mathbf{z}) + C_{F;ULS} P_{F;ULS}(\mathbf{z}) + C_{F;SLS} P_{F;SLS}(\mathbf{z}) \\
 \text{s.t. } z_i^L &\leq z_i \leq z_i^U \quad i = 1, \dots, m \\
 P_{F;ULS}(\mathbf{z}) &\leq P_{F;ULS}^U \\
 P_{F;SLS}(\mathbf{z}) &\leq P_{F;SLS}^U
 \end{aligned} \tag{5-25}$$

In which:

$\mathbf{z} = (z_1, z_2, \dots, z_m)$: The vector of design variables;

$C_T(\mathbf{z})$:	The total lifetime costs of the structure;
$C_I(\mathbf{z})$:	The investment in the structure as a function of the design variables \mathbf{z} ;
$C_{F;ULS}$:	The damage in monetary terms in case of ULS failure;
$C_{F;SLS}$:	The damage in monetary terms in case of SLS failure;
$P_{F;ULS}(\mathbf{z})$:	The probability of ULS failure as a function of the design variables;
$P_{F;SLS}(\mathbf{z})$:	The probability of SLS failure as a function of the design variables;
z_i^L, z_i^U :	The lower and upper bound of design variable i ;
$P_{F;ULS}^U, P_{F;SLS}^U$:	The upper bound of the failure probability for ULS failure and SLS failure respectively.

Generally the design variables will be subjected to constraints. For instance, all geometrical quantities should be greater than zero. Furthermore, the failure probabilities can be subject to constraints, especially for structures where human lives are involved. In that case the maximum failure probabilities are enforced by regulations. In cases that loss of human lives is not involved in case of failure of the structure, formally the constraint on the failure probabilities can be set to 1 and the acceptable failure probability as well as the optimal design are completely decided by the lifetime costs only. If relevant, maintenance costs and inspection costs can be added to the total expected lifetime costs.

Obtaining accurate assessments of the damage in case of failure is not always practically possible. In that case, the optimal design can be found by minimising a cost function which only comprises the investment and imposing a constraint on the failure probability which expresses a qualitative idea of the economic optimal failure probability.

If the design is performed using a code based partial safety factor system, the following optimisation problem is applicable:

$$\begin{aligned}
 \min_{\mathbf{z}} C_T(\mathbf{z}) &= C_I(\mathbf{z}) \\
 \text{s.t.} \quad z_i^L &\leq z_i \leq z_i^U \\
 G_i(\mathbf{z}, \mathbf{x}^c, \boldsymbol{\gamma}) &> 0
 \end{aligned} \tag{5-26}$$

In which:

$C_I(\mathbf{z})$:	The investment in the structure as a function of the design variables \mathbf{z} ;
$G_i(\mathbf{Z}, \mathbf{X}^c, \boldsymbol{\gamma})$:	The limit state function for failure mode i as a function of the design variables \mathbf{z} , the characteristic values of the random variables

as defined in the partial safety factor system \mathbf{x}^c and the vector of partial safety factors $\boldsymbol{\gamma}$.

Generally, partial safety factors are available for several target probabilities of failure or safety classes (see below). Since the choice of the safety factors involves implicitly the choice of a target probability of failure and expected costs of failure, the same optimal design should be obtained from (23) and (24).

5.2.7.2 Cost optimisation

If loss of life in case of failure of the structure is not an issue for the structure under consideration, no constraint is set on the failure probability and the acceptable probability of failure equals the economic optimal probability of failure. A procedure for probabilistic optimisation of vertical breakwaters has been developed (Sørensen et al, 1994; Voortman et al, 1998, Volume II, section 4.1).

The optimisation for a vertical breakwater can be written as:

$$\min_{\mathbf{z}} C(\mathbf{z}) = C_{I;0} + C_I(\mathbf{z}) + \sum_{n=1}^N \left(\frac{365C_{F;SLS}P_{F;SLS}(\mathbf{z}) + C_{F;ULS}P_{F;ULS}(\mathbf{z})}{(1+r'-g)^n} + \frac{C_{maint}}{(1+r')^n} \right) \quad (5-27)$$

$$\text{s.t. } 0 \leq z_i$$

In which:

- \mathbf{z} : The vector of design variables;
- $C_{I;0}$: Initial costs, not depending on the design variables;
- $C_I(\mathbf{z})$: Construction costs as a function of the design variables;
- $C_{F;SLS}$: Costs per day in case of serviceability failure;
- $P_{F;SLS}(\mathbf{z})$: The probability of serviceability failure per day;
- $C_{F;ULS}$: Costs per event in case of ultimate limit state failure;
- $P_{F;ULS}(\mathbf{z})$: The probability of ultimate limit state failure per year;
- C_{maint} : Maintenance costs for the breakwater per year;
- r' : The net interest rate per year;
- g : The yearly rate of economical growth, expressing growth and development of the harbour;
- N : The lifetime of the structure in years.

Inspection of Equation (5-27) shows that the total lifetime costs consist of investment costs and the expected value of the damage costs. In principle, for every year of the structure's lifetime, the expected damage has to be taken into account. Not all the costs are made at the same time. Therefore, the influence of interest, inflation and economical growth has to be taken into account in order to make a fair comparison of the different costs (van Dantzig, 1956).

The expected value of the damage costs is a function of the failure probability. The failure probability is a function of the design variables. Therefore, minimisation of Equation (5-27) results in the optimal geometry and at the same time the

optimal failure probability. Ready at hand minimisation algorithms can be applied to find the optimal set of design variables.

When implementing the cost function in any programming language, the failure probability as a function of the design variables has to be included. For this part of the cost function one of the probabilistic procedures introduced in section 5.2.3 or section 5.2.5 can be used. Due to the specific character of the optimisation process, the choice of the probabilistic procedure is not an arbitrary one. One should be aware of the following points:

- The minimisation process comprises a large number of evaluations of the cost function, each evaluation involving a probability calculation. Therefore, time-consuming methods should be avoided;
- The values of the cost function for any given point should be stable. Especially the Monte Carlo procedure provides probability estimates that contain an error, which is inherent to the procedure. This (small) error generally presents no problem, but in this case it causes variations of the cost function, which disturb the optimisation process (see Fig. 5-5).

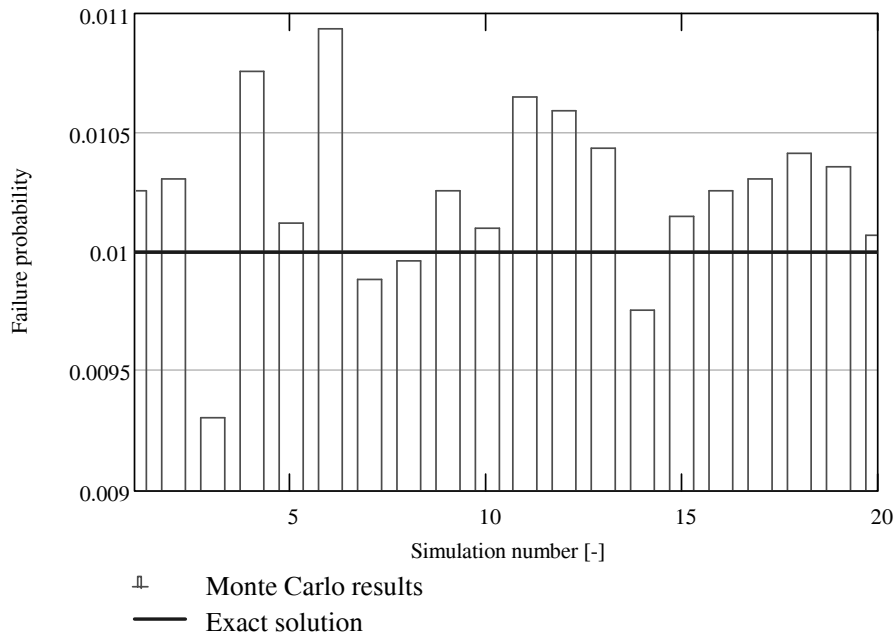


Figure 5-5. Result of 20 calculations of failure probability by Monte Carlo.

The points of attention mentioned above lead to the conclusion that level II methods are suitable for application in an optimisation process. Level III methods

will generally lead to too much computational effort or will disturb the optimisation process.

The procedure described above has been applied to a fictitious design case of a vertical breakwater in a water depth of 25 m. Three design variables are considered: the height and width of the caisson and the height of the rubble berm.

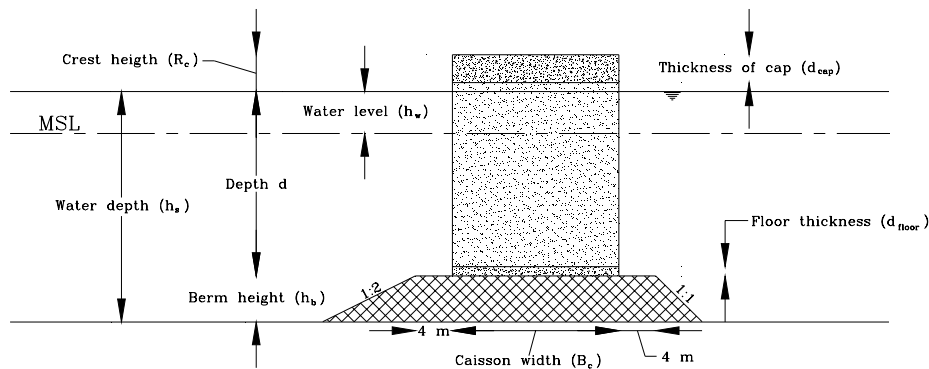


Figure 5-6: Overview of conceptual breakwater design for economic optimisation.

As a first step a deterministic optimisation for chosen wave heights has been performed. This step is meant to show the connection between the deterministic optimisation for a given safety level and the full probabilistic approach. Because of this, the choice of the input values (comparable to the characteristic values in Equation 5-26) is not corresponding to the choice made for the partial safety factor system (see below). Furthermore, all safety factors have been set to 1 and the berm height is fixed at a value of 6 m. For this situation it is possible to find a minimum caisson width as a function of the crest height for every single failure mode. Once the crest height and the caisson width are known, the construction costs of the caisson breakwater can be calculated (see Fig. 5-7).

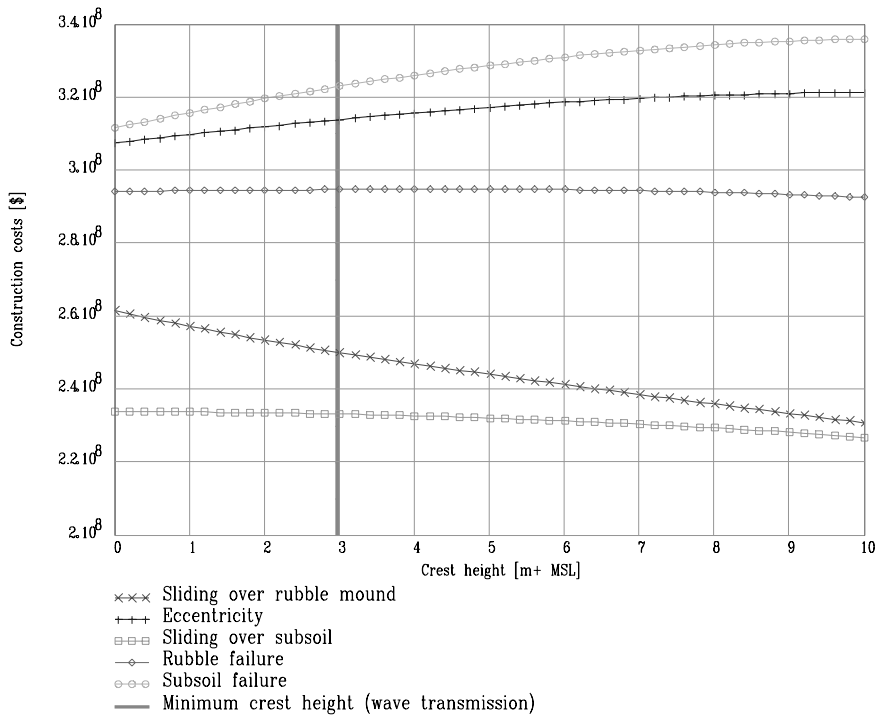


Figure 5-7. Construction costs of the breakwater as a function of the crest height (Berm height 6 m).

Generally, bearing capacity failure of the subsoil shows the largest minimum caisson width. Furthermore, the results show that in general a lower crest height leads to a more narrow caisson and thus to lower construction costs. However, the minimum crest height required is determined by wave transmission. In the deterministic approach the minimum crest height related to wave transmission imposes a constraint on the crest height. Thus, the optimal geometry is decided by wave transmission and by bearing capacity failure of the subsoil.

While at first sight it seems reasonable to have an equal failure probability of failure for all the failure modes in the system, probabilistic optimisation shows that, like in the deterministic approach, bearing capacity failure of the subsoil largely determines the probability of ultimate limit state failure (see Figure 5-8).

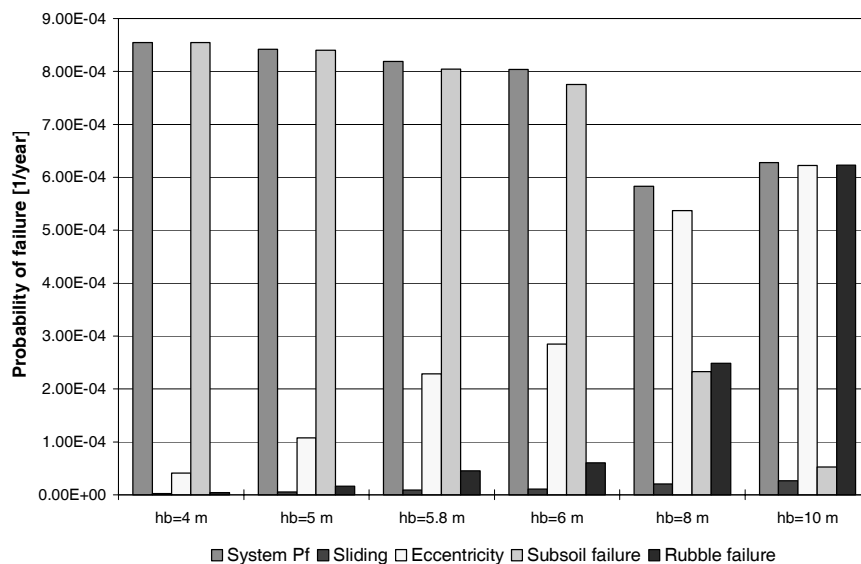


Figure 5-8. Overview of ULS failures probabilities for several berm heights.

Inspection of the lifetime costs as a function of crest height and caisson width indicates that also in the probabilistic approach the crest height is limited by wave transmission (see Fig. 5-9).

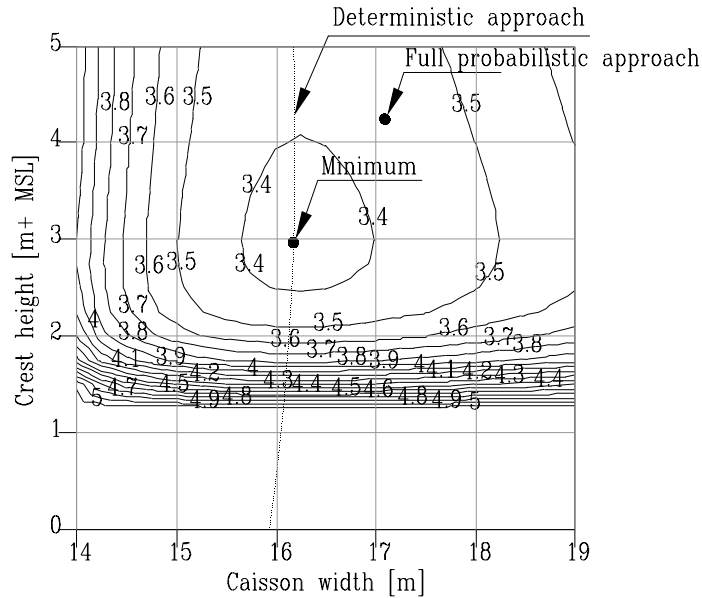


Figure 5-9. Contour plot of total lifetime costs in 10^8 US \$ (Random wave height only) and optimal geometries for different levels of modelling. Taken from Voortman et al (1998) (see also Volume IId, section 4.1).

The optimal probability of system failure is quite low in comparison to existing structures ($8 \cdot 10^{-4}$). This could be caused by the choice of the cost figures or by a limited spreading of the random variables.

5.2.7.3 Partial Safety Factor System

Partial safety factors used in design of vertical wall breakwaters can be calibrated on a probabilistic basis. The calibration is performed for a given class of structures, materials and/or loads in such a way that for all structure types considered the reliability level obtained using the calibrated partial safety factors for design is as close as possible to a specified target reliability level. Procedures to perform this type of calibration of partial safety factors are described in for example Thoft-Christensen & Baker, 1982, Madsen et al. (1986) and Ditlevsen & Madsen (1996).

A code calibration procedure usually includes the following basic steps:

- 1) definition of scope of the code; here : vertical wall breakwaters
- 2) definition of the code objective; here : to minimise the difference between the target reliability level and the reliability level obtained when designing different typical structures using the calibrated partial safety factors

- 3) selection of code format, see below
- 4) selection of target reliability levels, see section 5.2.6
- 5) calculation of calibrated partial safety factors, see below
- 6) verification of the system of partial safety factors, see below

The partial safety factors can be calibrated as follows. For each failure mode one or more limit state functions are established:

$$g_i(\mathbf{x}, \mathbf{z}) = 0 \quad (5-28)$$

where $\mathbf{x} = (x_1, \dots, x_n)$ are realisations of n stochastic variables $\mathbf{X} = (X_1, \dots, X_n)$ and $\mathbf{z} = (z_1, \dots, z_N)$ are the deterministic design variables.

Corresponding to (5-26) a design equation is established from which $\mathbf{z} = (z_1, \dots, z_N)$ are determined:

$$G_i(\mathbf{x}^c, \mathbf{z}, \gamma) = 0 \quad (5-29)$$

where $\mathbf{x}^c = (x_1^c, \dots, x_n^c)$ are characteristic values of $\mathbf{X} = (X_1, \dots, X_n)$ and $\gamma = (\gamma_1, \dots, \gamma_M)$ are partial safety factors. Usually design values for loads are obtained by multiplying the characteristic with the partial safety factors and design values for resistances are obtained by dividing the characteristic values with the partial safety factors. On the basis of the limit state functions in (1) element reliability indices β_i or a system reliability index β_s can be determined for the structure considered, see e.g. Madsen et al. (1986).

The partial safety factors γ are calibrated such that the reliability indices corresponding to L example structures are as close as possible to a target reliability index β^t . This is formulated by the following optimisation problem

$$\min W(\gamma) = \sum_{i=1}^L w_i (\beta_i(\gamma) - \beta^t)^2 \quad (5-30)$$

where $w_i, i = 1, 2, \dots, L$ are weighting factors indicating the relative frequency of appearance of the different design situations. Instead of using the reliability indices in Equation 5-30 to measure the deviation from the target, the probabilities of failure can be used. $\beta_i(\gamma)$ is the system reliability index for example structure i with a design \mathbf{z} obtained from the design equations using the partial safety factors γ and the characteristic values. Usually the partial safety factors are constrained to be larger than or equal to 1.

The code format and thus the partial safety factors to be used in design of vertical breakwaters can in principle depend on:

- a) the uncertainty related to the parameters in the relevant limit states
- b) the safety class
- c) the type of limit state
- d) the expected lifetime of the structure
- e) if laboratory model tests have been performed
- f) the amount of quality control during construction

Ad a) uncertainty related to parameters: the uncertainties related to the parameters in the limit state functions are taken into account in a deterministic design through partial safety factors. The partial safety factors are calibrated in such a way that a large partial safety factor is used in the case of large uncertainties and a small partial safety factor is used when the uncertainties are relatively small.

Ad b) safety class: the safety classes in section 5.2.6 are used.

Ad c) type of limit state: two types of limit states are considered, namely: ULS (Ultimate Limit State; e.g. foundation failure, failure of significant part of caisson concrete structure) and SLS (Serviceability Limit State, e.g. overtopping, settlement of foundation soil). Acceptable probabilities of failure could be as indicated in Table 5-4.

Ad d) expected lifetime: the expected lifetime T_L for vertical breakwaters can be quite different. Therefore three different expected lifetimes are considered: $T_L = 20$ years, $T_L = 50$ years and $T_L = 100$ years.

Ad e) model tests: sometimes laboratory tests are performed in order to estimate the wave loads more accurately. In that case the uncertainty related to the wave loads is reduced and it is therefore reasonable to decrease the partial safety factors. Similarly, also detailed field and laboratory tests are performed to determine the soil parameters. In that case the uncertainty related to the soil strength parameters is usually reduced and the partial safety factors can be reduced.

Ad f) quality control: finally, the uncertainty can also be dependent on the amount of control at the construction site.

The characteristic values are suggested to be the mean value for self weight and permanent actions, for wave heights the expected largest significant wave height in the design lifetime T_r , 5 % fractiles for structural strength parameters and the mean values for geotechnical strength parameters.

An example of the partial safety factor system is shown in Table 5-5.

Table 5-5. Partial safety factors.

p.s.f.	Parameter	Tentative values - γ
Loads		
γ_{G_1}	Self weight	1.0
γ_{G_2}	Permanent actions, e.g. ballast	1.1
γ_H	Wave load	See below
Strength		
γ_ϕ	Effective friction angle	See below
γ_{C_u}	Undrained shear strength	See below
γ_c	Concrete strength	1.6
γ_r	Reinforcement	1.3
γ_{scour}	Scour failure	See below
γ_{armour}	Armour layer failure	See below

The partial safety factor for the wave load is determined from :

$$\gamma_H = \gamma_{H_0} \gamma_T \gamma_{H_2} \tag{5-31}$$

Where:

γ_{H_0} takes into account the uncertainty related to the wave load

γ_T takes into account the influence of the expected lifetime. For example $\gamma_T=1$ for $T=50$ years, $\gamma_T > 1$ for $T=100$ years and $\gamma_T < 1$ for $T=20$ years.

γ_{H_2} takes into account the effect of model tests used to estimate the wave load. $\gamma_{H_2}=1$ if no model tests are performed

For partial safety factor for the geotechnical parameters are determined from :

$$\gamma_m = \gamma_0 \gamma_1 \gamma_2 \gamma_3 \tag{5-32}$$

Where:

γ_0 takes into account the uncertainty related to the strength parameter

γ_1 takes into account the effect of safety class. $\gamma_1=1$ for normal safety class

- γ_2 takes into account the effect of model tests used to estimate the strength parameters. $\gamma_2=1$ if no model tests are performed
- γ_3 takes into account the amount of control. $\gamma_3=1$ if normal control is used.

The factors in equations (5-31) and (5-32) are calibrated using representative values for the soil strength parameters and with wave climates from Bilbao, Sines, Tripoli and Fallonica (see Volume IId, section 4.2). The full stochastic model used in the calibration is shown in Table 5-5.

The calibrated partial safety factors corresponding to normal safety class in ULS and high safety class in SLS:

Wave load:	$\gamma_{H0}=1.1$
Effective friction angle:	$\gamma_0=1.2$
Undrained shear strength:	$\gamma_0=1.3$
Scour failure:	$\gamma_0=2.2$
Armour layer failure:	$\gamma_0=0.6$

The following factors defined in are derived (no factors are derived for γ_2 taking into account the effect of model tests used to estimate the strength parameters and γ_3 taking into account the amount of control). The factors for γ_1 can be used to obtain partial safety factors for all safety classes in ULS and SLS.

Table 5-6. Safety factor γ_T , which takes into account the influence of the expected lifetime T .

T	20 years	50 years	100 years
γ_T	0.98	1.0	1.05

Table 5-7. Safety factor γ_{H_2} that takes into account the effect of model tests used to estimate the wave load.

Model	1	2
γ_{H_2}	1.0	0.85

Table 5-8. Safety factor γ_I , which takes into account the effect of the safety class.

	Safety class				
	ULS	Low	Normal	High	Very high
SLS	Low	Normal	High	Very high	
P_f	0.4	0.2	0.1	0.05	0.01
γ_1	0.75	0.9	1.0	1.1	1.25

The safety classes correspond to the ones given in Table 5-5. The verification of the partial safety factors is described in Volume IId, section 4.2.

5.3 PROBABILISTIC METHODS APPLIED TO VERTICAL BREAKWATERS IN GENERAL

5.3.1 *Fault tree for a vertical breakwater*

As stated in section 5.2.2 the first step in developing the fault tree and the limit states for a structure is defining the functions that are to be performed. In this project the main function of a breakwater has been defined as:

"Providing sufficiently tranquil water for ship manoeuvring and berthing"

There are several ways in which a breakwater might fail to fulfil this main function. This could be caused by wave energy entering the harbour through the entrance by refraction and diffraction, wave energy passing over the breakwater due to severe overtopping or collapse of a part of the structure, leading to a breach. Wave energy entering through the entrance is a matter of design of the layout of the entrance and is not part of PROVERBS. It is however part of the system of failure modes and is therefore included in the fault tree. In this section only the top part of the fault tree is presented. The complete fault tree is given in section 4.2 of Volume II.

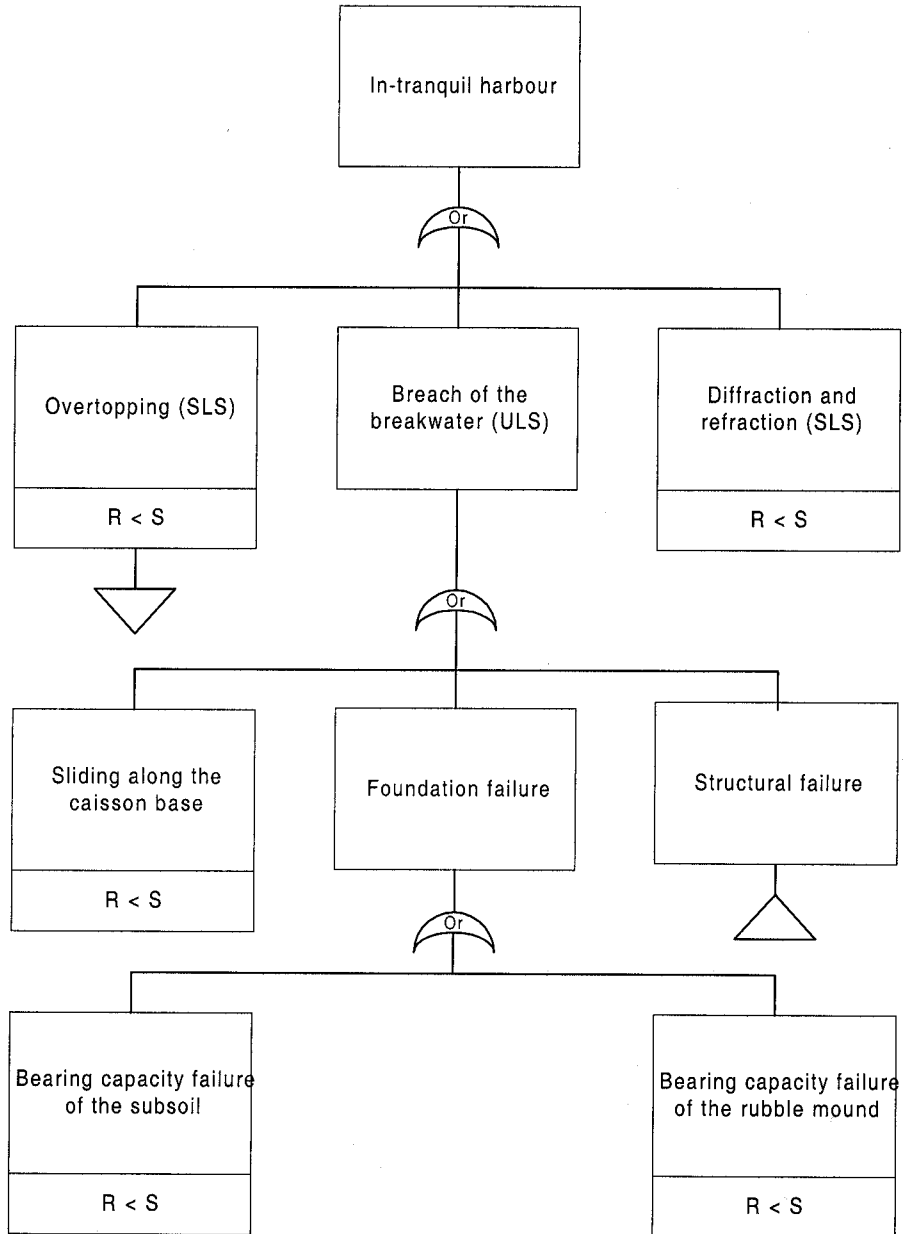


Figure 5-10. Fault tree of a vertical breakwater.

5.3.2 *Specific limit states for vertical breakwaters*5.3.2.1 *Introduction*

For a vertical breakwater several limit states can be discerned. Within PROVERBS an extensive set of failure modes has been created. This set consists of Ultimate as well as Serviceability Limit States. Accidental Limit States have been omitted.

5.3.2.2 *Loading of the breakwater*

For all limit states except wave transmission, the loading is given by the wave forces exerted at the breakwater. Within PROVERBS, extensive research has been directed to this aspect of breakwater design (details are given in Chapter 2). In the description given here, the emphasis is laid on the implementation of the load models in a probabilistic framework.

The models used in PROVERBS can be categorised in three types:

1. Load models describing quasi-static (pulsating) wave loads;
2. Load models describing dynamic (impact) wave loads;
3. Decision models, indicating what type of load model should be applied.

On a deterministic level, the parameter map and the breaker model (Volume IIa, sections 2.2 and 2.3) indicate the occurrence of impacts. In reality, the input to these models (water levels, wave properties) is of random nature. A general vertical breakwater will therefore encounter quasi-static loads as well as impact loads during its lifetime. Theoretically, the distribution function of all the wave loads exerted at the breakwater is therefore written as:

$$P(F < f) = P_{\text{impact}} \cdot P(F < f | \text{impact}) + (1 - P_{\text{impact}}) \cdot P(F < f | \text{no impact}) \quad (5-33)$$

In which:

- F : Wave load modelled as a stochastic variable
 P_{impact} : The probability of occurrence of impacts;
 $P(F < f | \text{impact})$: The distribution function of impact loads, conditional on the occurrence of impacts;
 $P(F < f | \text{no impact})$: The distribution function of pulsating wave loads, conditional on the occurrence of quasi-static loads, e.g. obtained by the model of Goda (1985).

The complex nature of especially the models for impact loading has led to the choice of Monte Carlo simulation for the risk analysis of breakwaters in conditions where impact loads might occur. For organisational reasons, in the probabilistic framework an early version of the model described in Chapter 2 of this Volume has been adopted. What has not been implemented is the distinction of steep

and flat bed slopes and the position of the breaker line. Omitting these parts of the impact model will generally lead to conservative estimates of the wave forces.

5.3.2.3 Serviceability limit states related to performance of the breakwater

Generally, breakwaters are built to provide protection against waves. Beside collapse of the breakwater itself, the breakwater can fail to provide protection because of refraction and diffraction effects or due to wave transmission. Refraction and diffraction should be limited by the design of the layout of the breakwater and the harbour entrance. Wave transmission has particularly influence on the cross section of the breakwater.

Wave transmission over vertical breakwaters can be described by means of the model of Goda (1969), modified for different caisson shapes by Heijn (1998).

The limit state for wave transmission has been defined as:

$$g(\mathbf{x}) = H_{s,acc} - K_t H_s \quad (5-34)$$

In which:

- $H_{s,acc}$: The acceptable significant wave height inside the harbour basin;
- K_t : Transmission coefficient calculated by the Goda-Heijn model (Goda, 1969, Heijn, 1998);
- H_s : Significant wave height on the sea side of the breakwater.

5.3.2.4 Foundation limit states

The geotechnical failure modes have been defined and formulated in Chapter 3. In short the failure modes are:

- Sliding along the base of the caisson;
- Bearing capacity failure of the rubble mound;
- Bearing capacity failure of the subsoil.

The limit state equations describing the different forms of failure are available on two levels of sophistication (see Chapter 3). In this section the set of limit state equations for preliminary design are adopted as the standard form of modelling the foundation. However, a comparison with other levels of modelling will be shown.

The general form of the foundation limit states is similar to the general form given in section 5.2.2. It is typical for foundation limit states that loading and strength can not always be completely separated. For instance, the weight of the caisson acts as a load but at the same time increases the effective stress in the foundation, thus increasing the shear strength. Next to the stress level, the strength of the foundation is primarily decided by the properties of the soil, such as the friction angle and the cohesion. An overview of the input for the soil models as well as the uncertainties related to the soil properties is given in Chapter 3.

5.3.2.5 *Structural limit states*

Like the modelling of the foundation, also the structural limit states of vertical breakwaters can be defined on different levels of sophistication (see Chapter 4). In principal, only the beam models given in Chapter 4 are suitable for application in a probabilistic calculation. A detailed description of these models is given in Chapter 4. The structural strength of the breakwater is primarily decided by the material properties, as well as the sizing of the elements. It is important to note that processes like chloride ingress or cracking of the concrete may lead to corrosion of the reinforcement, which lowers in the strength in time.

5.4 CASE STUDIES

5.4.1 *Genoa Voltri (Italy)*

5.4.1.1 *The case*

Voltri breakwater represents a typical Italian and European design. It is an existing breakwater that is supposed to be rather safe; the supposition is based on experience on similar and smaller breakwaters existing in Genoa since more than 40 years that suffered no damage; many other breakwaters, similar in shape and design criteria, are present in several harbours in Italy. The assessed failure probability (related to a lifetime of 50 years) can then be confronted with evidence in prototype conditions.

Information required for the analysis regards structure geometry, wave climate, foundation characteristics and construction method. Being a real breakwater an interpretation of available documents was necessary. As long time passed since design and construction, some information might have been lost or misinterpreted. Results are the best we could obtain within the project deadline, but no responsibility is assumed on them.

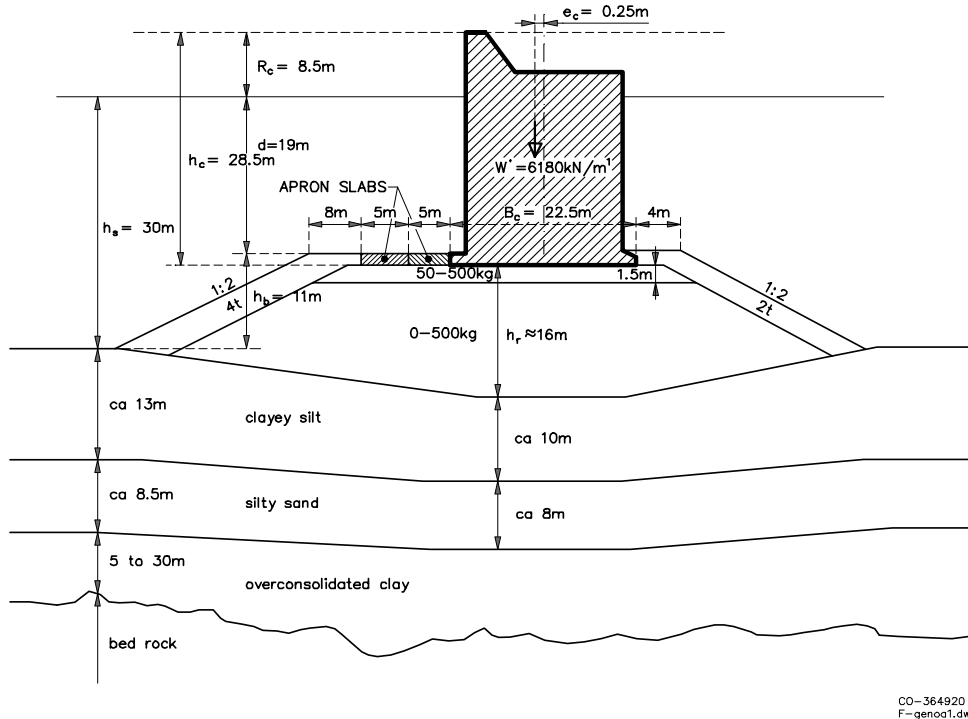


Figure 5-11. Breakwater section and soil layers in Voltri.

5.4.1.2 Wave forces

Breaking wave conditions were in principle excluded at design time by assuring a sufficient water depth in front of the wall; in order to verify the effect of this assumption breaking conditions are regarded as possible and the related hazard is analysed.

In most part of the analysis non breaking conditions are considered and the two set of formulae given by Goda (1985) are used in order to transform waves from off-shore to the structure site and to evaluate the maximum equivalent static force.

As the wave increases, breaking conditions may be reached. In breaking conditions the equivalent static force is computed using the new set of formulae developed within PROVERBS. The parameter map (Section 2.2.2) is used in order to understand which is the typical wave action that characterises the site. For the case of Voltri the parameter map shows that breaking waves are possible only for extreme wave conditions. Breaking wave height is evaluated according to (Section 2.2.3) and from this the percentage of waves breaking at the structure. Due to foreshore water depth the percentage of broken waves is negligible.

The force time pattern is evaluated on the basis of few parameters (Section 2.5.1), whose probability distribution was assessed by Van Gelder (1998) with the help of a data base of measures obtained by several physical models. The longitudinal extension of the breaker is considered to be the full caisson length (Section 2.5.3).

The dynamic model, developed and calibrated on the basis of prototype measurements carried out on a few caissons (Vol. II-b, Chapter 3), is used to evaluate the sliding force response factor, depending essentially on the ratio between force duration and relevant natural oscillation period; static equivalent horizontal and vertical force are then obtained.

Even for the same incident wave, breaking or non breaking conditions correspond to quite different static equivalent applied forces; the level II risk analysis procedure is unable to cope with this discontinuous behaviour. A level III analysis (Monte Carlo simulation) was then performed applying the model for breaking waves.

A level II analysis was anyway performed for the subset of non breaking conditions: the discontinuity was artificially removed extending the validity of the Goda formulae. The design point was found to be actually below the breaking limit. The complete validity of the non breaking hypothesis is confirmed by the comparison of the assessed failure probability with the Monte Carlo simulation in dynamic conditions.

5.4.1.3 *Failure functions*

Among the failure modes developed under PROVERBS (Vol. II-b Ch. 6), those related to caisson, rubble-mound and cohesive soil interaction were implemented; the relative failure probability is computed through a level II analysis.

The following failure modes are analysed by failure functions representing static force balance:

- caisson sliding along the base;
- bearing capacity failure in rubble mound, i.e. sliding within rubble mound (this mode dominates systematically the traditional overturning failure mode);
- bearing capacity failure in subsoil, i.e. sliding through the high rubble foundation and the silt-sand subsoil.

The analysis can not be considered exhaustive, since several failure modes were not implemented (settlement, scour, deterioration and corrosion of reinforcement due to chloride ingress through the concrete or through cracks, structural failure due to wave loading) and some hydraulic responses were not analysed (overtopping, wave transmission, wave reflection).

Some failure modes are limit sub-cases of others: Rubsan2 is a sub-case of Rubsand4, and Slidclay3 of Rubclay8. When model errors are not considered in

system hazard assessment, we can examine all of them at the same time and include them in the list of series element of the system. When model uncertainties are described only the best model is used for each failure mode (Rubsand4 and Rubclay8).

The system reliability is analysed and the lower bound and upper bound of the system failure probability are assessed with Ditlevsen method.

Bishop method is used as alternative to Rubsand4-Ruclay8 series to represent foundation stability, accounting for friction and cohesion in the rubble mound and for the likely configuration of the rubble-mound subsoil interface.

In dynamic conditions Monte Carlo simulations were carried out only for the sliding failure, the typical failure mode induced by breaking waves, Oumeraci (1994).

5.4.1.4 *Variable statistics*

In principle all the parameters are stochastic variables in a hazard analysis, but some show very small variation and can be considered as deterministic with almost no effect on the final result. These are almost all the geometric parameters and unit weights and a few others.

The shape of the statistical distribution of variable parameters is frequently known a-priori based on wider experience and on the nature of the variable. For instance the mean water level is the sum of a random meteorological effect and several sinusoidal astronomical components; the result is well described by a Gaussian variable.

The offshore significant wave height follows an extreme distribution which was better identified on the basis of the available dataset. Despite the importance of the harbour and probably due to the pluri-secular qualitative experience instrumental wave records are not available for Genoa. Wave measurements were sporadic and not public. The assumed statistics is based on KNMI visual observation and MetOffice hindcasting and is confronted with the qualitative experience, as described in Martinelli (1998). The offshore significant wave height was adapted to a GEV distribution (and resulted almost equivalent to a Gumbel distribution).

In all the cases where the variables were physically limited at one side, it was chosen to assume the LogNormal distribution associating null probability below the physical limit. For most cases the variance is small and the assumed distribution becomes almost equal to the Normal distribution.

When there was no clear information on the variance but only on reasonable extreme values, the simple rule was adopted that two standard deviations account for the difference between the maximum (minimum) and the mean value.

The assumed statistics for parameters relative to the hydraulic aspects is:

Table 5-9. Statistics for hydraulic boundary conditions for Genoa Voltri breakwater

GENOA VOLTRI (50 years)	Distribution	Mean value	Standard dev.	Notes
Off-shore significant wave height H_{os}	Gumbel	6.2 m	12%	Based on experienced storms
Deep water wave steepness s_{op}	LogNormal	0.035	10%	Based on steepness of most severe storms
Water level on M.S.L.	Normal	0.1 m	0.2 m	HHW=0.5 m

The statistics of geotechnical parameters assumed for Voltri is:

Table 5-10. Statistics of geotechnical parameters for Genoa Voltri breakwater

GENOA VOLTRI	Distribution	Mean value	Standard dev.	Notes
Sliding coefficient μ	LogNormal	0.64	10%	Takayama & Ikeda (1992); $\mu-2\sigma=0.5$
Rubble mound friction angle	Sum of two LogNormals	$E(\phi_{1r}+\psi_1)$	$\sigma(\phi_{1r}+\psi_1)$	$\mu-2\sigma=38^\circ$
Rubble mound residual friction angle, ϕ_{1r}	LogNormal	28°	2°	
Rubble mound dilation angle, ψ_1	LogNormal	16°	2°	
Rubble mound cohesion, for use in Coh-sand2*	LogNormal	20 kPa	10%	Japanese praxis, Tanimoto & Takahashi (1994)
Cayey silt cohesion	LogNormal	110 kPa	30%	$\mu-2\sigma=50$ kPa
Silty sand friction angle, ϕ_2	Sum of two LogNormals	$E(\phi_{2p}+\psi_2)$	$\sigma(\phi_{2r}+\psi_2)$	$\mu-2\sigma=27^\circ$
Silty sand residual friction angle, ϕ_{2r}	LogNormal	25°	2°	
Silty sand dilation angle, ψ_2	LogNormal	8°	2°	
Silty sand undrained cohesion	LogNormal	190 kPa	30%	Estimated from vertical pressure

The statistics of the main geometrical stochastic parameters influencing the resistance of the foundation is:

Table 5-11. Statistics for geometric parameters governing the resistance of the structure

<i>GENOA VOLTRI</i>	<i>Distribution</i>	<i>Mean value</i>	<i>Standard dev.</i>	<i>Notes</i>
Differences in super-structure thickness	Shifted LogNormal	2.2 m	0.25 m	Minimum value 1.0 m
Depth reached by rubble mound below original bottom, used with Bishop failure function	LogNormal	6.0 m	1.0 m	Evaluation of settlement performed before construction

5.4.1.5 Model uncertainties

In the attempt of finding all the sources of uncertainty, models and formulae used in the computations were examined and the effect of assumptions and approximations estimated.

Some models are physically based; variables involved are well known and no relevant error is associated to them. This is for instance the case of the formula that evaluates the caisson weight starting from the dimensions and the specific weights.

Some models (e.g. the Goda set of formulae for the evaluation of the maximum force and moments) are based on empirical relations and show a certain scatter (See Vol. IId, Section 4.1).

Other models (e.g. the geotechnical models) are physically based but rely on assumptions or simplifications; in this case an idea of the induced bias and uncertainty was obtained by applying different models.

In any case a calibration factor is applied to the result of the formula providing the true value. This factor is a random variable whose statistics represents bias and uncertainty of the formula.

Uncertainties in Goda wave force formulae

Goda formulae as most design formulae are biased in order to provide a safe relation, rather than the mean value; this must be accounted for in a reliability analysis.

Van der Meer et al. (1994) gave an estimate of the bias and standard deviation of the Goda formulae on the basis of model tests. Vrijling (1996) pointed out how the derived standard deviation included also statistical uncertainty of the maximum wave height in the experiment realisation. Vrijling arrived to the conclusions presented in the following table.

Table 5-12. Calibration factors for wave loading derived for the Goda model

<i>GODA Model</i>	<i>Distribution</i>	<i>Mean value</i>	<i>Standard dev.</i>	<i>Notes</i>
Calibration factor for horizontal forces	LogNormal	0.90	0.20	IId, Section 4.1
Calibration factor for uplift forces	LogNormal	0.77	0.20	IId, Section 4.1
Calibration factor for horizontal moments	LogNormal	0.72	0.37	IId, Section 4.1
Calibration factor for uplift moments	LogNormal	0.72	0.34	IId, Section 4.1
Calibration factor for seepage horizontal force	LogNormal	0.65	0.30	On the basis of the uncertainties given above

An analysis of the effect of apron slab provides results consistent with calibration factors reported in the table. Depending on gaps between the apron slabs, under-pressure can be smaller than predicted by Goda formula and, due to uncertainty of the spatial distribution, its shape is not always triangular. The uncertainty of moments is slightly greater than the uncertainty of forces.

The great uncertainty is mainly related to breaking waves conditions. Several model tests show that if the formula is restricted to non breaking waves the standard deviation is much lower (6-8% for horizontal force).

The statistics of the calibration factor for seepage forces, not defined by Goda's formulae nor checked by van der Meer or Vrijling, was derived from the linear pressure distribution suggested by Goda. The effect of a filtration length longer than the caisson base is greater on seepage forces than on uplift, the bias and uncertainty of this calibration factor are therefore assumed proportionally greater than for uplift.

For the breaker impact model we assume the statistics presented by van Gelder (1998):

Table 5-13. Statistics for stochastic parameters in the impact model

	<i>Distribution</i>	<i>Mean value</i>	<i>Standard dev.</i>	<i>Notes</i>
Coefficient 'k' for impulse of breaking wave	LogNormal	0.086	97%	Van Gelder (1998)
Coefficient 'c' for total duration of breaking wave force	LogNormal	2.17	50%	Van Gelder (1998)

Uncertainties in geotechnical failure functions

For all geotechnical models the calibration factor Z is assumed as homogeneous to a failure load (or safety) factor: the failure function has always the form $R/S-Z$. Definitions of resistance R and load S and statistics for Z are provided below.

The effect of approximations and hypotheses were roughly evaluated assuming that the foundation geometry is correctly schematised by the failure functions.

The most realistic failure functions based on the upper limit theory are credited of a 2% average error towards the unsafe side. A similar error is credited to Bishop method, Lancellotta (1995).

The effect of friction among the unstable body and the adjacent stable ones is evaluated assuming horizontal pressure equal to 60% of the vertical pressure. Under non breaking waves it is assumed that instability is extended to a 100 m long reach of the breakwater, whereas under breaking waves it is assumed that instability regards a single caisson.

Table 5-14. Calibration factors for various failure modes in the subsoil incl. uncertainties

<i>Failure function</i>	<i>Definition of the calibration factor</i>	<i>Expected value</i>	<i>Uncertainty</i>	<i>Comments</i>
Slidtak1	$(F_G - F_U) \tan \phi / F_H$	1.00	1%	Horizontality err.
RubSand2	$\{W_{i+} + (F_G - F_U) \omega_{1V} / \{ (F_H + F_{HU}) \omega_{1H} \}$	1.10 1.05	10% 15%	Non breaking Breaking
CohSand2	$\{W_{int} + W_{i+} + (F_G - F_U) \omega_{1V} / \{ (F_H + F_{HU}) \omega_{1H} \}$	1.10 1.05	10% 15%	Non breaking Breaking
SlidClay3	$W_i / (F_H + F_{HU})$	0.96 0.85	4% 10%	Non breaking Breaking
Rubsand4	$\{ \Sigma W_{i+} + (F_G - F_U) \omega_{1V} / \{ (F_H + F_{HU}) \omega_{1H} \}$	0.97 0.87	3% 8%	Non breaking Breaking
RubClay8	$\{ \Sigma W_{i+} + (F_G - F_U) \omega_{4V} / \{ (F_H + F_{HU}) \omega_{4H} \}$	0.96 0.85	4% 10%	Non breaking Breaking
Bishop	M_R / M_S	0.97 0.87	3% 10%	Non breaking Breaking

5.4.1.6 *System failure probability*

The considered failure modes are caisson sliding, rubble mound and subsoil failure. Failure probabilities and design point co-ordinates are given in the following table.

Table 5-15. Genoa Voltri hazard analysis for separate modes.

Failure function	Failure prob. In 50 years	<i>Design point of main variables</i>				
		H_{so}	Sliding coefficient μ	Rubble mound friction angle ϕ_1	Rubble mound cohesion	Cohesion subsoil c_u'
Slidtak1	2.3%	7.6 m	0.60			
Rubsand2	8.0%	7.0 m		43.0°		
CohSand2	2.9%	7.5 m		43.0°	19.8 kPa	
Rubsand4	11.5%	6.8 m		43.0°		
Slidclay3	8.2%	6.8 m		43.6°		84.1 kPa
RubClay8	8.1%	6.8 m		43.5°		83.6 kPa
Bishop	1.5%	7.8 m		42.8°	19.8 kPa	110.0 kPa

Since model errors are considered, only the best equation (equation providing the least uncertainty) is used for each independent failure mode in system failure analysis. We judged that Slidtak1 is representative of caisson sliding over the base, Rubsand4 of rubble mound bearing capacity failure and Rubclay8 of subsoil bearing capacity failure. The overall failure probability results to be 15% (the lower and upper bounds are 14.7% and 15.2% respectively). The value should be taken as typical for structures of this kind recently designed in Europe.

Rubsand4, i.e. bearing capacity failure in rubble mound causing sliding along a curved surface, results to be the most important failure mode. This does not agree with the experienced failures (see for instance Oumeraci, 1994) since failure in the rubble mound is not commonly reported as a cause of breakwater failure (not as much as sliding at the caisson base). This could be due in some proportion to the specific design of Voltri rubble mound, that is evidently less wide at the harbour side than at the offshore side, or possibly to an erroneous evaluation of calibration factor statistics, for instance to an underestimation of systematic effect of lateral friction, or else this failure mode that can represent an important horizontal displacement of caissons can be confused in prototype with caisson sliding on its base.

The design wave conditions correspond actually to non breaking waves.

5.4.1.7 Sensitivity analysis

A sensitivity analysis of failure probability showed that future wave load is the greatest cause of uncertainty; second is the complex of model uncertainties and third foundation characteristics.

The effect of the berm width at the harbour side was analysed showing that a wider berm would result in a significantly safer breakwater.

The effect of a real or apparent (representing the curvature of the failure boundary) cohesion in the rubble mound shows that even a smaller value than suggested by Japanese guidelines (12 compared to 20 kPa) combined with a cautious tangent friction angle of 35° result in a significantly stronger rubble mound than for the equivalent secant friction angle 37° (8.2 % against 12.8 % failure probability).

Similarly the use of Bishop failure function combined with a realistic curved contact surface between rubble mound and subsoil shows that failure probability estimated by Rubclay8 for a conventional geometry (plane horizontal base) is significantly overestimated. As a consequence the system failure probability should be controlled by rubble mound failure more than shown by previous figures.

5.4.1.8 *Effect of breaking*

A Monte Carlo simulation was performed including the effect of possible breaking waves for sliding failure mode. In extreme conditions breakers do actually occur but failure probability does not increase since caisson would slide yet for lower non breaking waves. A similar result occurs obviously also for the critical rubble mound failure mode, showing that globally breaking even if possible does not influence the hazard of the analysed breakwater.

5.4.1.9 *Conclusions*

- The structure failure probability was found to be around 10-15%.
- The critical failure mode is bearing capacity failure in the rubble mound.
- A wider berm at the harbour side would significantly reduce the hazard.
- The greater hazard originates from the intrinsic uncertainty of future waves.
- Uncertainty in Goda formulae is relevant, but relevance would decrease if the better behaviour of the formulae for non breaking waves is considered.
- Different model uncertainties, both for wave action and for foundation behaviour, should be applied for non breaking and breaking waves.

5.4.2 *Easchel breakwater*

5.4.2.1 *Introduction*

The Easchel breakwater is a fictitious breakwater, placed on a thin bedding layer. The sea bottom consists of well-described Eastern Scheldt sand. The objective of this case study is twofold:

304 Probabilistic Design Tools for Vertical Breakwaters

1. Investigate the influence of a few geometric parameters of the breakwater on the probability of caisson instability (sliding along the base, bearing capacity failure of the rubble mound, bearing capacity failure of the subsoil);
2. Investigate the influence of model variations on the probability of caisson instability.

Ad 1: The width of the caisson and the height of the top slab have been varied. The results lead to a modification of the original design;

Ad 2: For the modified design, the following variations of models have been studied:

- Two different models for wave breaking (Goda and linear wave theory);
- Two alternatives for the loading of the breakwater (including or neglecting of impacts, see Chapter 2);
- Two alternatives for the probability calculations (First Order Reliability Method or Monte Carlo, this chapter)
- Foundation modelling on three levels of sophistication (feasibility level design, preliminary design and finite element modelling, see also Chapter 3).

In this case study all failure probabilities are expressed per year.

5.4.2.2 Breakwater geometry and boundary conditions

The Easchel breakwater is built on a mildly sloping seabed. The slope equals 0.4% for a long distance offshore. The depth at the toe is 12.6 m with respect to mean sea level. An overview of the breakwater cross section is given in Figure 5-12.

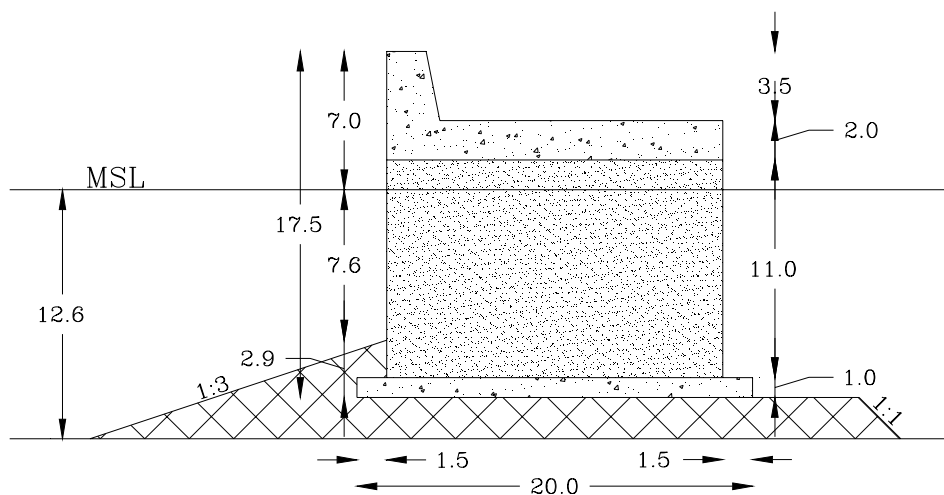


Figure 5-12. Overview of breakwater cross section.

The subsoil consists of Eastern Scheldt sand, which was thoroughly investigated in the design phase of the Eastern Scheldt Storm Surge Barrier in the Netherlands. For the properties of the rubble, expert estimates have been used.

Table 5-16. Overview of distributions of rubble properties.

<i>Variable</i>	<i>Distribution type</i>	<i>Mean</i>	<i>Standard deviation</i>
Friction angle	Normal	43	2.5
Dilatancy angle	Lognormal	10	1.4
Density	Deterministic	21	-
Cohesion	Deterministic	0	-

Table 5-17. Overview of distributions of subsoil properties.

<i>Variable</i>	<i>Distribution type</i>	<i>Mean</i>	<i>Standard deviation</i>
Friction angle	Normal	37	2
Dilatancy angle	Lognormal	8	1.4
Density	Deterministic	21	-
Cohesion	Deterministic	0	-

The hydraulic boundary conditions are given in Table 5-18.

Table 5-18. Overview of hydraulic boundary conditions on deep water.

<i>Variable</i>	<i>Distribution type</i>	<i>Mean</i>	<i>Standard deviation</i>
Water level (h_w)	Normal	0.2	0.2
Significant wave height (H_{s0}) [m]	Gumbel	5.05	0.63
Wave steepness (s_{0p}) [-]	Lognormal	0.027	0.0068

The breakwater is placed in an area with a negligible tidal difference. A small variation of the water level has been assumed.

Generally, the wave height and the wave period are highly correlated. In a probabilistic calculation this correlation has to be taken into account. A description of the correlation by means of a physical relationship is generally to be preferred. Analysis of buoy measurements shows that the equivalent deep water wave steepness, defined as:

$$s_{0p} = \frac{H_{s0}}{\frac{g}{2\pi} T_p^2} \tag{5-35}$$

is virtually statistically independent of the wave height. Therefore, the wave steepness has been used as input in the probabilistic calculation and the wave period is derived from the wave height and the wave steepness.

5.4.2.3 *Inshore wave climate*

For the reliability analysis, the wave conditions just in front of the breakwater are relevant. Several models for wave transformation in shallow water have been proposed (Goda, 1985; Vrijling & Bruinsma, 1980; Battjes & Janssen, 1978). In this study the model of Goda and the model of Vrijling & Bruinsma (denoted as the Eastern Scheldt model) have been used. A sample of 10.000 wave heights is shown in Figure 5-13.

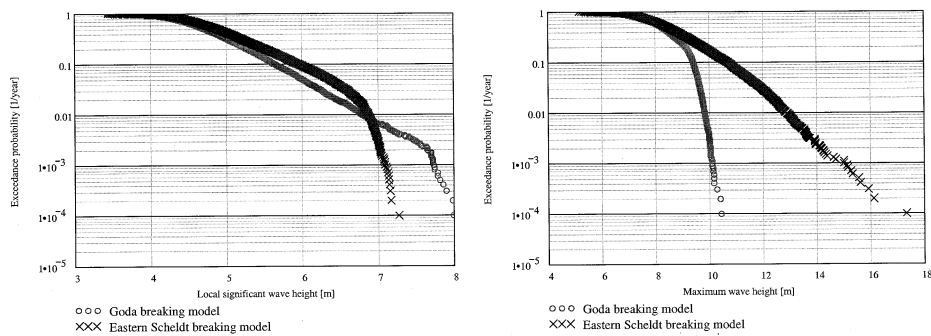


Figure 5-13. Empirical distributions of significant wave height and maximum wave height in front of the breakwater.

It appears that the Goda model results in slightly higher significant wave heights in front of the structure. However, the maximum wave heights, which are relevant for the force calculations, are higher for the Eastern Scheldt model. Analysis showed that the differences regarding the maximum wave height may be caused by one parameter which is chosen as a fixed value in the Goda model and which is treated as a random variable in the Eastern Scheldt model (Volume IId, section 5.2).

5.4.2.4 *Loading of the structure*

The loading of the structure has been determined in two different ways:

- According to the classical Goda model, including the model uncertainty derived by Bruining (1994);
- According to the model developed in the PROVERBS project, as described in Chapter 2.

The combination with the wave transformation model leads to a total of four alternative force distributions. The resulting horizontal forces are shown in Figure 5-14.

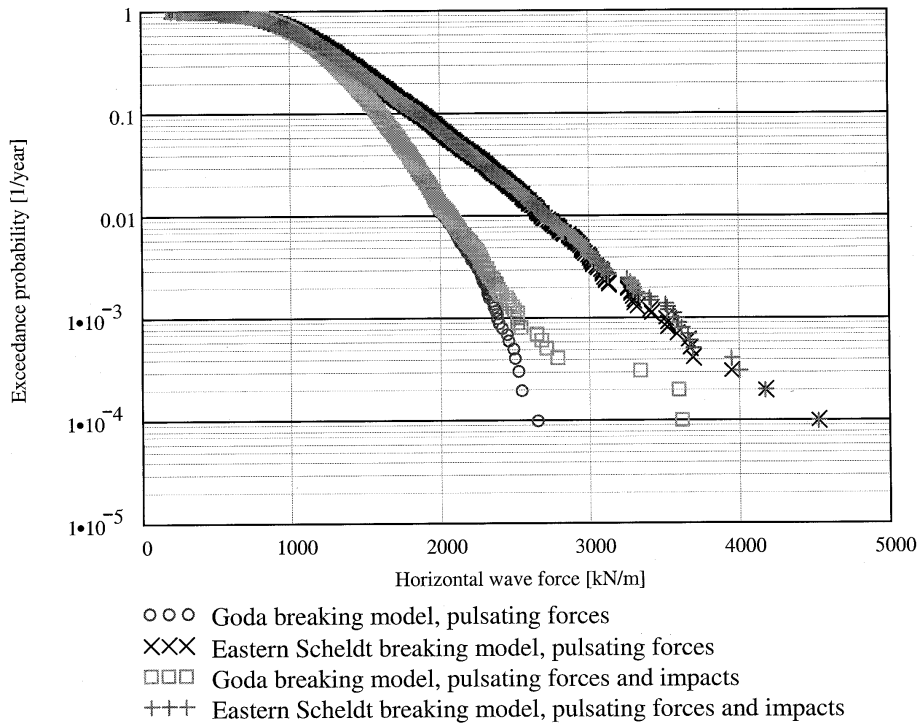


Figure 5-14. Empirical distributions of horizontal wave force for four model combinations.

For pulsating forces only, the influence of the higher maximum wave heights resulting from the Eastern Scheldt model is clearly visible. In case of the Goda wave breaking model, application of the impact model leads to an increase of the forces in the upper region of the distribution. In case of the Eastern Scheldt model the influence on the horizontal force is small. The influence is mainly found in the region around the 10^{-3} quantile. Since this is in the order of magnitude of the failure probability of the structure, application of the impact model does influence the failure probability in case of the Eastern Scheldt breaker model (see below).

5.4.2.5 Influence of the breakwater geometry on the probability of caisson instability

The influence of the caisson width and the thickness of the top slab have been investigated for the model combination Goda wave breaking / pulsating forces. The influence of the caisson width is shown in Figure 5-15.

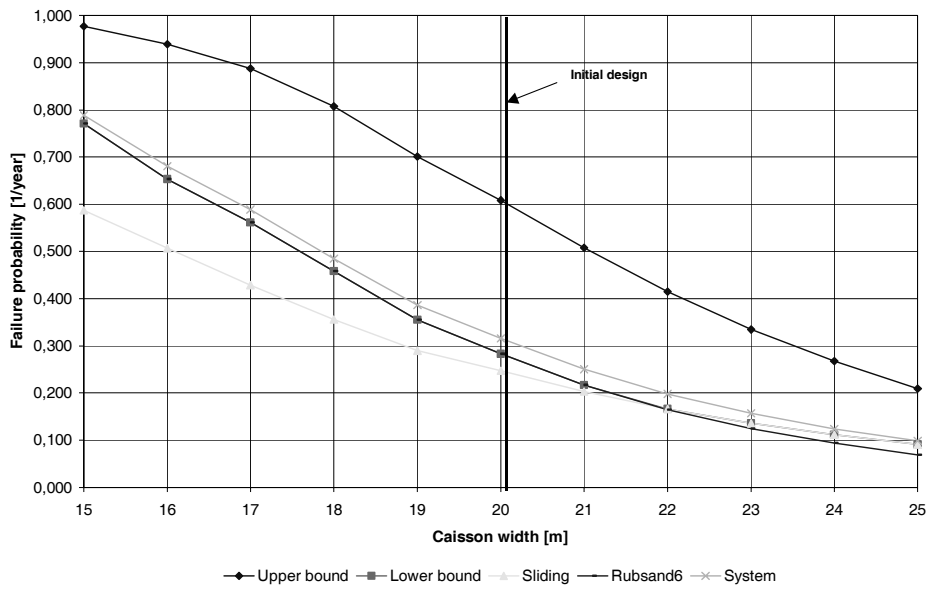


Figure 5-15. Influence of caisson width on the probability of caisson instability.

The top slab thickness is varied in such a way that the crest height of the breakwater remains constant, i.e. the crown wall is stepwise replaced by a thicker top slab. Figure 5-16 shows the resulting probability of caisson instability.

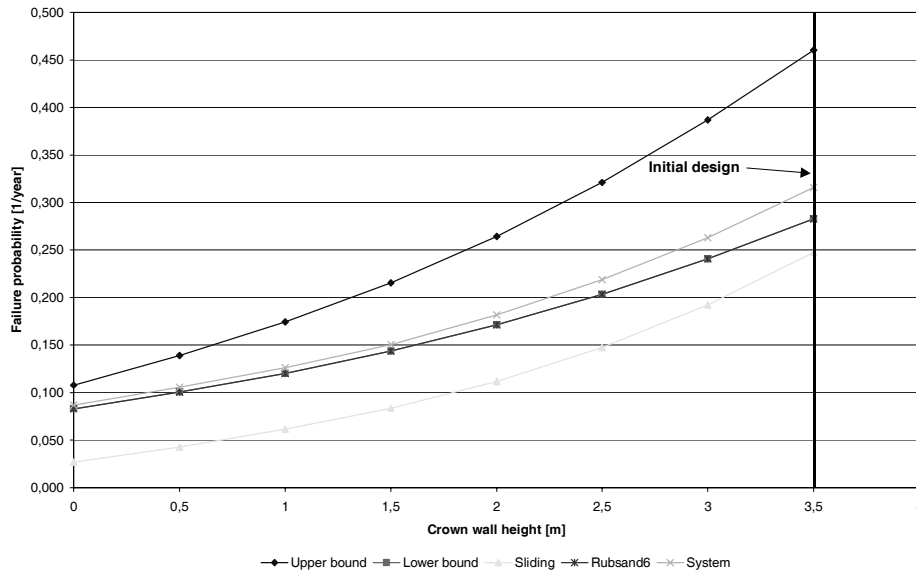


Figure 5-16. Influence of the top slab thickness on the probability of caisson instability.

The results of the sensitivity analysis lead to a modification of the design. See Figure 5-17.

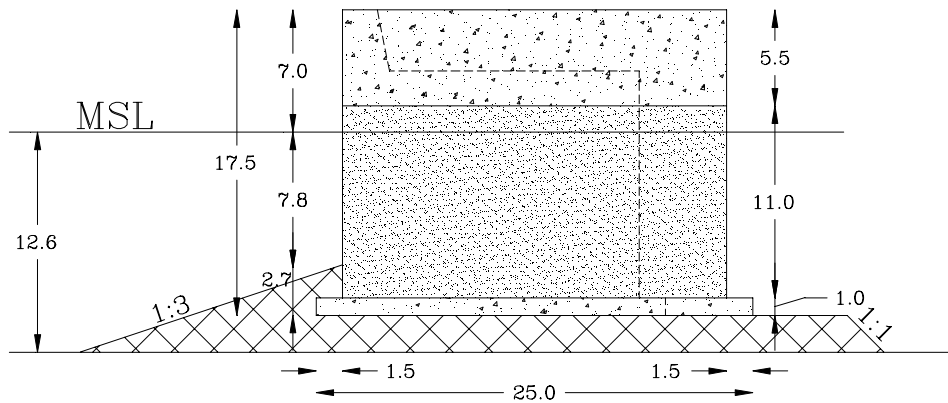


Figure 5-17. Cross section of the modified design of the Easchel breakwater (dotted line: original design).

5.4.2.6 Comparison of model combinations for pulsating wave loads

For pulsating loads, eight model combinations have been used. An overview is given in Table 5-19.

Table 5-19. Overview of tested model combinations for quasi-static loads.

No.	Foundation model	Wave breaking model	Integration method
1	Preliminary	Goda	FORM
2			Monte Carlo
3		Eastern Scheldt	FORM
4			Monte Carlo
5	Feasibility	Goda	FORM
6			Monte Carlo
7		Eastern Scheldt	FORM
8			Monte Carlo

An overview of the results is given in Figure 5-18.

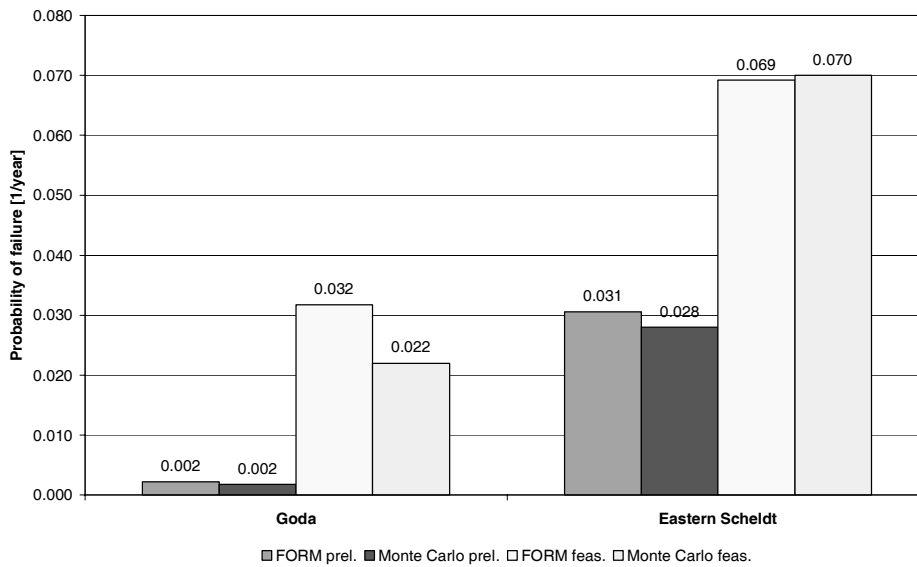


Figure 5-18. Overview of calculated failure probabilities for different combinations of calculation method and foundation models (pulsating forces only).

As expected, the feasibility design level models for the foundation tend to be more conservative than the preliminary design level models. This results in higher failure probabilities for this type of foundation models. Furthermore, the higher maximum wave heights for the Eastern Scheldt model lead to higher fail-

ure probabilities. Generally, the calculated failure probability is in the same order of magnitude for FORM and Monte Carlo.

Using the design points from the FORM calculations in a finite element model (PLAXIS) supports the conclusion that the feasibility models are the most conservative. The PLAXIS results show that the feasibility models underestimate the wave load at collapse by approximately 30 % (compared to PLAXIS) and the preliminary design models by approximately 10 % (Volume IId, section 5.2).

5.4.2.7 *The influence of impact loading*

The probability of failure under impact loading has been calculated using Monte Carlo analysis. As expected, application of impact loading leads to an increase of the failure probability.

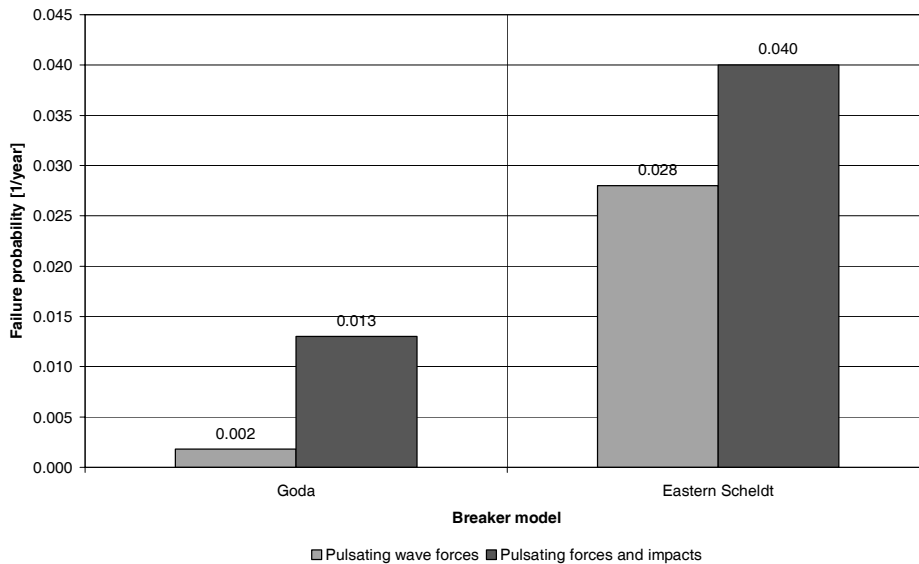


Figure 5-19. Calculated failure probabilities for pulsating loads and for mixed loading (calculation method: Monte Carlo, Foundation model: preliminary design level).

5.4.3 *Reliability analysis of geotechnical failure modes for the Mutsu-Ogawara West breakwater*

5.4.3.1 *Introduction*

A reliability analysis is performed with a breakwater with the same geometry as the Mutsu-Ogawara West breakwater in Japan. The geometry is shown in Figure 5-20. The wave conditions and the subsoil strength parameters are not known

such that a detailed stochastic model for these can be formulated. Therefore a representative wave climate corresponding to the known design wave height is assumed. Further, weak and strong subsoil models are formulated which represent typical strength parameters for sand (drained) and clay (undrained) subsoils. The design lifetime is 50 years. In this case study all failure probabilities are expressed per lifetime (see Figure 6.5, page 119 in Christiani, 1997).

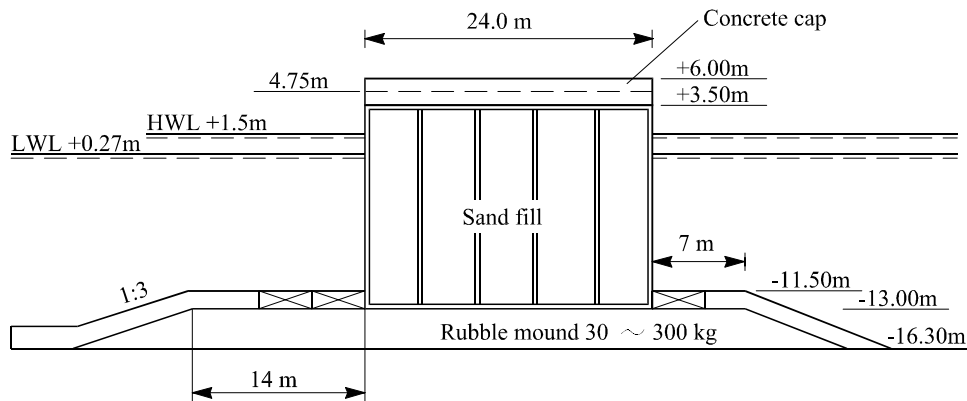


Figure 5-20. Mutsu-Ogawara breakwater.

5.4.3.2 Stochastic models

Wave height

The maximum significant wave height H_S^T in the design lifetime T is assumed to be modelled on the basis of a limited number N of wave height observations. An extreme Weibull distribution is used:

$$F_{H_S^T}(h) = \left[1 - \exp \left(- \left(\frac{h - H'}{u} \right)^\alpha \right) \right]^{\lambda T} \quad (5-36)$$

where λ is the number of observations per year. α , u and H' are parameters to be fitted to the observed data. In order to model the statistical uncertainty u is modelled as a Normal distributed stochastic variable with coefficient of variation

$$V_u = \frac{1}{\sqrt{N}} \sqrt{\frac{\Gamma(1+2/\alpha)}{\Gamma^2(1+1/\alpha)} - 1} \quad (5-37)$$

The design significant wave height is 8.0 m. It is assumed that $N = 20$ data has been used, $\lambda = 1$, $\alpha = 0.90$, $u = 1.71$ m and $H' = 0$ m.

The model uncertainty related to the quality of the measured wave data is modelled by a stochastic variable F_{H_S} which is assumed to be normal distributed with a coefficient of variation equal to 0.05 corresponding to good wave data.

Wave load

Both pulsating and impact wave loading are considered:

- ◆ Pulsating wave loads are estimated using the Goda formula, see section 2.4.1. The model uncertainties related to horizontal and uplift wave forces are assumed to be fully correlated. Also model uncertainties related to horizontal and uplift wave moments are assumed to be fully correlated.
- ◆ Impact loading consisting of a horizontal and a vertical (uplift) part is estimated by the model described in section 2.5.1. The model uncertainties related to the impact loads are described in detail in section 2.5.4 and modelled by the stochastic variables no. 18, 19, 20 and 21, see Table 5-20.

Geotechnical parameters

The geotechnical parameters for the rubble mound material and the subsoil are not known for the Mutsu-Ogawara breakwater. Therefore representative strength parameters are used corresponding to weak and strong subsoils. Both sand (drained) and clay (undrained) subsoil models are considered. Further different values of the coefficient of variation of the strength parameters are investigated, see Table 5-20. Since the undrained shear strength for clay is modelled by a stochastic field the correlation structure has to be specified. The expected value function $E[c_u(x, z)]$ and the covariance function $C[c_u(x_1, z_1), c_u(x_2, z_2)]$ are assumed to be:

$$E[c_u(x, z)] = c_{u0} + c_{u1}z \tag{5-38}$$

$$C[c_u(x_1, z_1), c_u(x_2, z_2)] = \sigma_{c_u}^2 \exp(-|\alpha(z_1 - z_2)|) \exp(-(\beta(x_1 - x_2))^2) \tag{5-39}$$

where (x_1, z_1) and (x_2, z_2) are two points in the soil. z is the vertical coordinate and x is the horizontal coordinate. $\sigma_{c_u} = 30$ kPa, $\alpha = 0.33 \text{ m}^{-1}$ and $\beta = 0.033 \text{ m}^{-1}$ are used. For weak clay : $c_{u0} = 79$ kPa and $c_{u1} = 1$ kPa/m. For strong clay : $c_{u0} = 173$ kPa and $c_{u1} = 0$ kPa/m. The statistical parameters for weak and strong sand subsoil can be seen in Table 5-20.

The complete list of stochastic variables is shown in Table 5-20.

314 Probabilistic Design Tools for Vertical Breakwaters

Table 5-20. Statistical model for Mutsu-Ogawara breakwater. W: Weibull, N: Normal, LN: Log-Normal.

i	X_i	Description	Mean	Standard Deviation	Distribution
1	H_S	Significant wave height [m]	see above	See above	W
2	u	Weibull parameter [m]	2	See above	N
3	F_{H_S}	Model uncertainty on wave height	1	0.05	N
4	s_M	Wave steepness factor	1	0.25	N
5	ζ	Tidal elevation, maximum $\zeta_0 = 0.8$ m			Cosine
6	U_{F_H}	Model uncertainty horizontal force	0.90	0.2	N
7	U_{F_U}	Model uncertainty uplift	0.77	0.2	N
8	U_{M_H}	Model uncertainty horizontal moment	0.81	0.40	N
9	U_{M_U}	Model uncertainty uplift moment	0.72	0.37	N
10	ρ_c	Average density of caisson [t / m ³]	2.23	0.11	N
11	ϕ_1	Effective friction angle - rubble mound	46°	4.6°	LN
12	ψ_1	Angle of dilation - rubble mound	16.7°	1.67°	LN
13	ϕ_2	Effective friction angle - sand subsoil	39.0°/42.8° weak/strong	3.9° / 4.3° weak/strong	LN
14	ψ_2	Angle of dilation - sand subsoil	10.2°/15.3°	1.0° / 1.5°	LN
15	U	Clay strength	1	0	N
16	f	Friction coefficient	0.636	0.0954	LN
17	c_u	Undrained shear strength for impact load	400 kPa	80 kPa	LN
18	k	Factor for impact load	0.086	0.084	LN
19	c	Factor for impact load	2.17	1.08	LN
20	R	Model uncertainty factor for impact rise time	1	0.3	LN
21	U_I	Model uncertainty factor for impact forces	1	0.5	LN

5.4.3.3 Reliability analysis

The failure modes described in section 5.3.2 are used and the probability of failure within the design lifetime T is estimated. Eleven limit state functions are formulated for the following failure modes:

- sliding :
 1. sliding along the caisson base
- Bearing capacity failure of the rubble mound:
 2. rupture in rubble along bottom of caisson
 3. rupture in rubble mound - straight rupture line
 4. rupture in rubble mound – curved rupture line
- Bearing capacity failure of the subsoil (sand)
 5. rupture in subsoil along bottom of rubble mound
 6. rupture in rubble mound and sand subsoil – mode 1
 7. rupture in rubble mound and sand subsoil – mode 2
- Bearing capacity failure of the subsoil (clay)
 8. rupture in subsoil along bottom of rubble mound
 9. rupture in rubble mound and clay subsoil – mode 1
 10. rupture in rubble mound and clay subsoil – mode 2

In the case of impact loads and sand subsoil, the subsoil is assumed to behave as undrained and the following failure mode is investigated:

- Bearing capacity failure of the subsoil (undrained, impact loads only):
 11. rupture in rubble mound and sand subsoil – mode 2

Tables 5-21 and 5-22 show the results of a reliability analysis of the breakwater. Three different coefficients of variation for the soil strength parameters are investigated. The reliability analysis is performed using Monte Carlo simulation with 10.000 samples. The system probability of failure is taken as the maximum probability of failure for the individual failure modes. It is seen that if impact loading is taken into account then the probability of failure is very high, especially for weak clay subsoil. Further it is also seen that for clay subsoil it is very important if the strength is weak or strong. The importance of the coefficient of variation of the soil strength is only important for strong clay subsoil. Finally, it is seen that reasonable low and acceptable probabilities of failure are obtained for strong subsoils if model tests to determine the wave loads more accurate are performed.

Table 5-21. Probability of failure in a lifetime of 50 years for sand subsoil.

Coeffi- cient of variation	No impact load				Impact load			
	No model tests		Model tests		No model tests		Model tests	
	Weak	Strong	Weak	strong	Weak	Strong	Weak	Strong
0.05	0.065	0.037	0.0023	0.0023	0.29	0.27	0.25	0.25
0.08	0.065	0.037	0.0023	0.0023	0.29	0.27	0.25	0.25
0.10	0.065	0.037	0.0023	0.0023	0.29	0.27	0.25	0.25
Probability of impact					0.26			

Table 5-22. Probability of failure in a lifetime of 50 years for clay subsoil.

Coeffi- cient of variation	No impact load				Impact load			
	No model tests		Model tests		No model tests		Model tests	
	Weak	Strong	Weak	Strong	Weak	Strong	Weak	Strong
0.10	0.71	0.027	Weak	0.0023	0.76	0.27	0.82	0.25
0.15	0.71	0.036	0.77	0.0037	0.76	0.27	0.80	0.25
0.20	0.71	0.051	0.74	0.0180	0.76	0.28	0.78	0.26
Probability of impact					0.26			

Table 5-23 shows the probability of failure for the different failure modes in the case of no impact loading taking into account and strong subsoil with coefficients of variation equal to 0.15 for clay and 0.08 for sand. It is seen that if no model tests are performed the most important failure modes are no. 7 (sand) and 10 (clay). If model tests are performed also failure mode 1 (sliding) can be important. In Volume IId, section 5.3, a more detailed description of the reliability analyses is given including a description of the most important stochastic variables.

Table 5-23. Probability of failure for the case of no impact loading and strong subsoil with coefficients of variation equal to 0.15 for clay and 0.08 for sand.

<i>Failure mode</i>	<i>no model tests</i>	<i>model tests</i>
1 rubble mound	$1.76 \cdot 10^{-2}$	$2.31 \cdot 10^{-3}$
2	$4.02 \cdot 10^{-4}$	$2.32 \cdot 10^{-7}$
3	$4.79 \cdot 10^{-3}$	≈ 0
4	$4.80 \cdot 10^{-7}$	≈ 0
5 sand subsoil	$2.00 \cdot 10^{-4}$	≈ 0
6	$2.31 \cdot 10^{-2}$	$1.00 \cdot 10^{-4}$
7	$3.73 \cdot 10^{-2}$	$3.00 \cdot 10^{-4}$
System / sand subsoil	$3.73 \cdot 10^{-2}$	$2.31 \cdot 10^{-3}$
8 clay subsoil	$1.12 \cdot 10^{-2}$	≈ 0
9	$1.63 \cdot 10^{-2}$	$2.00 \cdot 10^{-4}$
10	$3.62 \cdot 10^{-2}$	$3.70 \cdot 10^{-3}$
System / clay subsoil	$3.62 \cdot 10^{-2}$	$3.70 \cdot 10^{-3}$

5.5 PERSPECTIVES

5.5.1 Durability

An important consideration in the design of concrete structures in seawater is that of durability. Chloride ingress, thought to be aided by loading induced cracking of the concrete threatens the steel reinforcement. Over time, the cross-section of the reinforcement will be reduced by corrosion, spalling will take place and finally the strength of the concrete structure will be impaired.

Models to describe chloride ingress as a diffusion process are available. At this moment one has to rely however on measurements at the completed structure to estimate the necessary values of the diffusion coefficient. It is not yet possible to estimate these values just on the basis of the concrete specification.

Also models to estimate the rate of the corrosion and the related reduction of the size of the reinforcement still have to be developed. In practice this is solved by designing the reinforcement on the basis of SLS conditions and limited crack-width (typically 0.3 mm) with a safety factor of approximately 1.5. The result is that the ULS load can be easily withstood by the concrete structure and that the amount of reinforcement is decided by the limitation of the crack-width in the SLS condition.

To avoid uneconomic over-design, better models have to be developed that relate chloride ingress, which is thought to be accelerated by cracking, to the final failure of the structure with reduced reinforcement.

5.5.2 *Impacts*

The maximum force and the duration of impacts in prototype are still a matter of discussion. This will be solved by further research.

In the mean time a designer should try to avoid creating impact conditions in front of the vertical breakwater. A study of the parameter map (Chapter 2) shows that impact can mostly be avoided by choosing the appropriate geometry for the caisson and the mound on which it is founded.

5.5.3 *Construction*

When, during the design of a breakwater one is presented with the choice between a rubble mound type and a vertical caisson breakwater a thorough consideration of the construction method and sequence should be made. It is clear that the transport and the placement of huge caisson structures without proper consideration is more risky than the handling of classical armour elements on a rubble mound breakwater. Also unexpected settlements during construction are more easily accommodated by rubble mound structures than caisson structures.

5.5.4 *Reflection*

Without further measures, the reflection of the incoming waves by a vertical breakwater is nearly 100%, resulting in a confused sea in front of the structure that may cause hindrance to shipping. Perforating the front wall can to some extent reduce this effect. The effectiveness of the reduction for random seas with a peak frequency changing over time should be further studied.

5.5.5 *Shear keys*

A philosophy for the design of shear keys has to be developed. The central question is to what extent a caisson may call on his neighbours during ULS conditions in short crested seas. It should be noted that a large dependency on shear key action could lead to repeated movement of a single caisson during a subsequent wave crest and through

ACKNOWLEDGEMENTS

The following people are gratefully acknowledged for their contribution to this chapter:

H.F. Burcharth	Aalborg University, Denmark
J. Dalsgaard Sørensen	Aalborg University, Denmark
P.H.A.J.M. van Gelder	Delft University of Technology, The Netherlands
A. Lamberti	University of Bologna, Italy
L. Martinelli	University of Bologna, Italy

REFERENCES

- Andrews, J.D.; Moss, T.R. 1993. Reliability and risk assessment. Harlow, U.K.: Longman Scientific and Technical, 368 pp.
- Battjes, J.A.; Janssen, J.P.F.M. 1978. Energy loss and set-up due to breaking of random waves. *Proceedings International Conference Coastal Engineering (ICCE)*, Hamburg, Germany, no. 16, Volume 1, pp. 569-587.
- Breitung, K. 1984. Asymptotic approximations for multinormal integrals. *Journal of Engineering Mechanics*, ASCE, Engineering Mechanics Division, vol. 110, pp. 357-366.
- Bruining, J.W. 1994. Wave forces on vertical breakwaters. Reliability of design formula. *Delft Hydraulics Report*, Emmeloord, The Netherlands, 65 pp.
- Bucher, G.C. 1987. Adaptive sampling, an iterative fast Monte Carlo procedure. *Internal Report, University of Innsbruck*, Innsbruck, Austria.
- Christiani, E. 1997. Application of reliability in breakwater design. *Ph.D. thesis, Hydraulics & Coastal Engineering Laboratory, Department of Civil Engineering, Aalborg University*, Aalborg, Denmark, Series Paper 14, 179 pp.; 1 Appendix.
- CUR 1997. Risk analysis in civil engineering. *Centre for Civil Engineering Research, Codes and Specification*, CUR Research Committee E10 "Risk Analysis", no. 190, Vol. 1: Probabilistic Design in Theory, Gouda, The Netherlands. In Dutch.
- Ditlevsen, O. 1979. Narrow reliability bounds for structural systems. *Journal of Structural Mechanics*, vol. 7, pp. 453-472.
- Ditlevsen, O.; Madsen, H.O. 1996. Structural reliability methods. Chichester et al.: John Wiley & Sons, 372 pp.
- Enevoldsen, I.; Sørensen, J.D. 1993. Reliability-based optimisation of series systems and parallel systems. *Proceedings IFIP WG 7.5 Conference on Reliability and Optimisation of Structural Systems*, Thoft-Christensen, P.; Ishikawa, H., Takamatsu, Kagawa, Japan, no. 5, pp. 31-46.
- Eurocode 1 1994. Basis of design and actions on structures. Part 1: Basis of Design.
- Goda, Y. 1969. Re-analysis of laboratory data on wave transmission over breakwaters. *Report. Port and Harbour Research Institute (PHRI)*, Tokyo, Japan, vol. 8, no. 3.
- Hasofer, A.M.; Lind, N.C. 1974. An exact and invariant first order reliability format. *Journal of the Engineering Mechanics Division*, ASCE, vol. 100, pp. 111-121.
- Heijn, K.M. 1997. Wave transmission at vertical breakwaters. *Master Thesis, Delft University of Technology*, Delft, The Netherlands.
- Hohenbichler; Rackwitz, R. 1983. First-order concepts in system reliability. *Structural Safety*, vol. 1, pp. 177-188.

320 Probabilistic Design Tools for Vertical Breakwaters

- Lancellotta, R. 1995. Geotechnical engineering. Rotterdam, The Netherlands: Balkema, rev. and updated edition, 436 pp.
- Madsen, H.O.; Krenk, S.; Lind, N.C. 1986. Methods of structural safety. Englewood Cliffs, N.J., USA: Prentice Hall Inc., 403 pp.
- Martinelli, L. 1998. Risk analysis of Genoa Voltri breakwater: the case of Genoa Voltri. *Ph.D. Thesis, Università di Bologna*, 15 December 1998, Bologna, Italy.
- NKB 1978. Recommendations for loading and safety regulations for structural design. *NKB report*, no. 36.
- Oumeraci, H. 1994. Review and analysis of vertical breakwater failures - lessons learned. *Coastal Engineering, Special Issue on 'Vertical Breakwaters'*, Eds.: Oumeraci, H. et al., Amsterdam, The Netherlands: Elsevier Science Publishers B.V., vol. 22, nos. 1/2, pp. 3-29.
- Ouypornprasert, W. 1987. Adaptive numerical integration in reliability analysis. *Internal Report, University of Innsbruck*, Innsbruck, Austria.
- Schueller, G.I.; Stix, R. 1987. A critical appraisal of methods to determine failure probabilities. *Structural Safety*, Amsterdam, The Netherlands: Elsevier Science Publishers B.V., vol. 4, pp. 293-309.
- Sørensen, J.D.; Burcharth, H.F.; Christiani, E. 1994. Reliability analysis and optimal design of monolithic vertical wall breakwaters. *Proceedings IFIP WG 7.5 Conference on Reliability and Optimisation of Structural Systems*, Rackwitz, R.; Augusti, G.; Borri, A. (eds.), Assisi, Italy, no. 6, Part 2: Technical Contributions, Paper 27, pp. 257-264.
- Takayama, T.; Ikeda, N. 1992. Estimation of sliding failure probability of present breakwaters for probabilistic design. *Report. Port and Harbour Research Institute (PHRI)*, Tokyo, Japan, vol. 31, no. 5, pp. 3-32.
- Tanimoto, K.; Takahashi, S. 1994. Design and construction of caisson breakwaters - the Japanese experience. *Coastal Engineering, Special Issue on 'Vertical Breakwaters'*, Eds.: Oumeraci, H. et al., Amsterdam, The Netherlands: Elsevier Science Publishers B.V., vol. 22, nos. 1/2, pp. 57-77.
- Thoft-Christensen, P.; Baker M.J. 1982. Structural reliability theory and its applications. Berlin/Heidelberg/New York: Springer, 267 pp.
- Van Dantzig, D. 1956. Economic decision problem for flood prevention. *Econometrica*, vol. 24, pp. 276-287.
- Van der Meer, J.W.; d'Angremond, K.; Juhl, J. 1994. Probabilistic calculations of wave forces on vertical structures. *Proceedings International Conference Coastal Engineering (ICCE)*, ASCE, Kobe, Japan, vol. 23.
- Van Gelder, P.H.A.J.M. 1998. Analysis of wave impact data on vertical breakwaters. *Proceedings Task 4 Workshop, MAST III, PROVERBS-Project: Probabilistic Design Tools for Vertical Breakwaters*, Delft, The Netherlands, Version 27/28 August 1998, Annex IV, 4 pp.; 8 figs.
- Voortman, H.G.; Kuijper, H.K.T.; Vrijling, J.K. 1998. Economic optimal design of vertical breakwaters. *Proceedings International Conference Coastal Engineering (ICCE)*, ASCE, Copenhagen, Denmark, no. 26, 14 pp.
- Vrijling, J.K.; Bruinsma, J. 1980. Hydraulic boundary conditions. In: *Hydraulic aspects of coastal structures: Developments in hydraulic engineering related to the design of the Oosterschelde storm surge barrier in the Netherlands*, Delft, The Neth, pp. 109-133.
- Vrijling, J.K.; Van Hengel, W.; Houben, R.J. 1995. A framework for risk evaluation. *Journal of Hazardous Materials*, Amsterdam, The Netherlands: Elsevier Science B.V., vol. 43, pp. 245-261.
- Vrijling, J.K. 1996. Evaluation of uncertainties and statistical descriptions. *Proceedings Task 4 Workshop Hannover, MAST III, PROVERBS-Project: Probabilistic Design Tools for Vertical Breakwaters*, Annex 3, Hannover, Germany, 15 pp.; 1 Annex.

